UNIVERSITÀ
DEGLI STUDI
DI PADOVA

Università degli Studi di Padova

Dipartimento di *Scienze Chirurgiche, Oncologiche e Gastroenterologiche*

SCUOLA DI DOTTORATO DI RICERCA IN
ONCOLOGIA E ONCOLOGIA CHIRURGICA
XXVIII CICLO

THE ROLE OF NITRIC OXIDE IN CANCER IMMUNOTHERAPY

Direttore della Scuola: Ch.mo Prof. PAOLA ZANOVELLO

Supervisore: Ch.mo Prof. VINCENZO BRONTE

Co-supervisore: Dr. BARBARA MOLON

Dottorando: ANDRIELLY HENRIQUE ROCHA AGNELLINI

UNIVERSITÀ
DEGLI STUDI
DI PADOVA

Università degli Studi di Padova

Dipartimento di *Scienze Chirurgiche, Oncologiche e Gastroenterologiche*

SCUOLA DI DOTTORATO DI RICERCA IN
ONCOLOGIA E ONCOLOGIA CHIRURGICA
XXVIII CICLO

THE ROLE OF NITRIC OXIDE IN CANCER IMMUNOTHERAPY

Direttore della Scuola: Ch.mo Prof. PAOLA ZANOVELLO

Supervisore: Ch.mo Prof. VINCENZO BRONTE

Co-supervisore: Dr. BARBARA MOLON

Dottorando: ANDRIELLY HENRIQUE ROCHA AGNELLINI

Index

Abstract

The adoptive cell therapy (ACT) represents one promising and realistic strategy to treat cancer patients trough cancer immunotherapy. This clinical approach consists in the transfer of $CD8^+$ T lymphocytes, specific for tumor antigens. The effectiveness of ACT so far is limited by crucial events as the trafficking of adoptively transferred cells to the tumor site and the highly immunosuppressive environment of developing cancer.

Tumors are complex and flexible lesions where cancer cells and host immune cells dynamically interact. The immunosuppressive functions are exerted by distinct cell populations as myeloid derived suppressor cells (MDSCs) and tumor associated macrophages (TAMs) that are known to suppress T cell proliferation in several ways. One is based on the coordinated up regulation and activity of two specific enzymes: arginase (ARG1) and nitric oxide synthase type 2 (NOS2 or iNOS). At the tumor site, ARG1 induces the depletion of the amino acid L-arginine that is necessary for T cell activation and proliferation. NOS2 is responsible for the generation of nitric oxide (NO) and other reactive nitrogen species (RNS). These free radicals are known to impair T cell functions within the tumor. Additionally, our group recently described a novel tumor-associated immunosuppressive mechanism based on post-translational modifications of chemokines by RNS. NO has dual role in cancer biology because it can promote both tumor progression as well as tumor regression. NO induces tumor progression and metastasis by direct induction of tumor-cell proliferation, migration and invasion, and indirectly through the expression of angiogenic and lymphangiogenic factors in tumor cells. On the other hand, high doses of NO have cytotoxic effects, which can result in tumor regression and metastasis inhibition. This dichotomous behavior mainly depends on the quantity, location, and timing of NO production and on the cellular sensitivity to this radical.

The primary aim of the study was elucidate the role of NOS2 and its principal product NO in the tumor microenvironment and more specifically in the ACT approach. To this purpose, we performed *in vivo* experiments of ACT in either wild type or Nos2 knock-out mouse models, challenged with a tumor cell line expressing the OVA antigen. Instrumental for dissecting the role of NO in ACT was the setting of a valuable tools whether to monitor in real-time NO release by confocal microscopy on viable tumor slices after T cell interaction or sorting isolation of specific population responsible for NO induction after ACT.

Our study proposed an innovative approach to study NO dynamics within intact tumor microenvironment. Our approach was instrumental for the definition -for the first time in tumors- of a new subset of myeloid population, named TNF/iNOS producing dendritic cells (Tip-DCs), with antitumor activity mediated by NOS2 and consequently NO. Mostly important our study brought the awareness that NOS2 is fundamental for the effectiveness of ACT, opening new perspectives to improve cancer immunotherapy based on NOS2/NO modulation in tumors.

Riassunto

L'immunoterapia cellulare adottiva (indicata di seguito con l'acronimo inglese ACT) oggi rappresenta una promettente strategia per il trattamento di pazienti affetti da cancro. Quest'approccio clinico consiste nel trasferimento adottivo di linfociti T CD8+, specifici per gli antigeni tumorali. L'efficacia dell'ACT è limitata da alcuni eventi fondamentali come il richiamo delle cellule trasferite nel sito tumorale e l'ambiente molto immunosoppressivo in cui si sviluppa il cancro.
I tumori sono delle lesioni complesse e dinamiche, nelle quali le cellule neoplastiche interagiscono con le cellule del sistema immunitario dell'ospite. Nel tumore, l'immunosoppressione è mediata da alcune popolazioni cellulari come le cellule mieloidi e i macrofagi associati al tumore, noti per sopprimere la proliferazione delle cellule T in diversi modi. Uno di questi è la sovraespressione e l'attività coordinata di due enzimi: l'arginasi (ARG1) e l'ossido nitrico sintasi 2 (NOS2 o iNOS). Nel sito tumorale ARG1 induce la deplezione dell'aminoacido L-arginina, necessaria per l'attivazione e la proliferazione delle cellule T. NOS2 è responsabile della sintesi dell'ossido nitrico e altre specie reattive dell'azoto. Questi radicali liberi sono noti bloccare le funzioni delle cellule T nel tumore. Inoltre, il nostro gruppo recentemente ha descritto un nuovo meccanismo d'immunosoppressione associato al tumore basato sulle modifiche post-traduzionali indotte dalle specie reattive dell'azoto sulle chemochine. L'ossido nitrico ha un duplice ruolo nella biologia del cancro poiché può promuovere come inibire la progressione tumorale. L'ossido nitrico induce la progressione tumorale e le metastasi agendo direttamente sulla proliferazione e migrazione delle cellule tumorali e indirettamente attraverso l'espressione di fattori angiogenici e linfoangiogenici. Tuttavia, una elevata concentrazione di ossido nitrico può causare effetti citotossici che possono condurre alla regressione tumorale e l'inibizione delle metastasi. Questa dicotomia dipende principalmente dalla quantità, dalla localizzazione e dalla cinetica di generazione dell'ossido nitrico e soprattutto dalla sensibilità cellulare all'esposizione di questo radicale.
L'obiettivo primario di questo studio è stato di delucidare il ruolo di NOS2 e del suo principale prodotto (ossido nitrico) nel microambiente tumorale, in particolare nell'approccio clinico dell' immunoterapia cellulare adottiva. Abbiamo svolto esperimenti di trasferimento adottivo sia nel modello animale wild type che nel modello Nos2 knock-out, nei quali si è indotto lo sviluppo di tumori mediante l' inoculo di una linea tumorale esprimente l'antigene ovalbumina (OVA). Allo scopo di chiarire il ruolo dell'ossido nitrico nell'immunoterapia cellulare adottiva, si è rivelato fondamentale la messa a punto di valide metodiche per monitorare il rilascio di questo radicale in tempo reale attraverso la microscopia confocale, che è stata condotta su "fettine" vitali di tumore in seguito all'interazione con le cellule T e l'isolamento tramite delle cellule responsabili dell'induzione di ossido nitrico dopo l'immunoterapia cellulare adottiva.
Il nostro lavoro introduce un approccio innovativo per lo studio delle dinamiche dell'NO nel microambiente tumorale. Tale approccio è stato fondamentale per l'identificazione, per la prima volta nei tumori, di una nuova sottopopolazione mieloide, denominata "cellule dendritiche TNF/iNOS producenti" (Tip-DCs), caratterizzate da attività antitumorale che è mediata da NOS2 e conseguente produzione di ossido nitrico. Principalmente il nostro studio porta la consapevolezza che la NOS2 è fondamentale per l'efficacia dell'ACT, aprendo nuove prospettive per il miglioramento dell'immunoterapia del cancro basata sulla modulazione di NOS2 e dell'ossido nitrico nei tumori.

Introduction

Despite considerable progress in the last decades, cancer still represent one leading cause of death in modern society. In the last 20 years, the survival of cancer patients with conventional treatment remains around at 10%. This poor clinical outcome highlights the need for new therapeutic approaches, providing long-lasting protection against disease recurrence. One promising branch is represented by cancer immunotherapy, based on the activation of the host immune system against tumors.
Cancer immunotherapy encompasses different approaches as monoclonal antibody therapy, vaccines and adoptive cell therapy (ACT). Recent evidence suggests that the effectiveness of these new approaches relies on the capability of immune system to overcome the immunosuppressive tumor microenvironment. Since the cross-talk between immune cells and tumor mass is fundamental for the therapeutic outcome, the clarification of mechanisms that blocks immune system may represent a promising opportunity to improve the effectiveness of immunotherapies.

1. Cancer immunotherapy

The relationship between the immune system and human cancer is dynamic and complex. Individual human tumors harbour a multitude of somatic gene mutations and epigenetically dysregulated genes, which products could be potentially recognizable as foreign antigens (Segal et al., 2008). However, during tumor progression, immune cells establish a tolerance, where foreign molecules expressed by cancer cells are viewed as self (Schreiber et al., 2011). Cancer immunotherapy exploits distinct approaches as monoclonal antibody-based treatment, vaccines and ACT, to specifically activate both adoptive and innate responses against tumors. Here, we will briefly describe the first two approaches, mainly focusing on ACT, which will be the object of our study.

1.1 Monoclonal Antibody-based therapy and Cancer Vaccines

Monoclonal antibodies (mAbs) are currently used in clinical oncology for the treatment of hematologic and solid tumors (Topalian et al., 2011). The mechanisms of tumor cell killing by antibodies can be classified in three groups: i) direct tumor cell killing, ii) immune-mediated tumor cell killing and iii) vascular and stromal ablation. In the first group, tumor killing could be elicited by the activation or inactivation of a specific receptor on tumor cells leading to apoptosis; antibodies can also bind enzymes leading to neutralization, signaling abrogation and cell death (Scott, Wolchok, and Old 2012). Direct killing also include antibodies loaded with cytotoxic agents as drug, small interfering RNA or radioisotope. In the second group the tumor killing can be the result of phagocytosis, complement activation cytotoxicity (CDC), antibody-dependent cellular cytotoxicity (ADCC), target of T cell genetically modified, T cell activation mediated cross-presentation of antigen to dendritic cells and inhibition of T cell receptor inhibitory.
The third group is composed by antagonists or ligands trapping of vasculature's receptors, stromal cell inhibitors and of course the antibodies which deliver toxins to stromal cells (Scott et al., 2012).

Tumor cell killing trough CDC and ADCC is based on Fc function of antibodies as mediator; in fact, it was shown that patients with high affinity to Fc receptor had better response than patients with low affinity in treatment of lymphoma with rituximab, which is based on ADCC (Weng and Levy, 2003). Others approaches have been successfully applied in the clinic by many new drugs: the abrogation of tumor cell signaling (for example, by cetuximab and trastuzumab) (Hudis, 2007; Van Cutsem et al., 2009), and the immune modulation of T cell function (for example, by ipilimumab) (Hodi et al., 2010).

Although promising results from different trials, treating malignant patients with antibodies may not achieve an adequate therapeutic effect for the heterogeneity of target antigen expression in tumors, which can be present initially or can develop during therapy.

Therapeutic vaccines represent a valuable option for active immunotherapy of cancers (Guo et al., 2013). This approach induces or increases antitumor responses with optimal combinations of antigens, adjuvants and delivery vehicles (Melero et al., 2014). The mechanism required to mount an effective anti-tumor immunity is a multistep process. In the first step, tumor-associated antigens (TAAs) must be directly presented by tumor cells or captured, processed and presented by dendritic cells. The second step requires the efficient activation and/or maturation of specific signals that allow dendritic cells to differentiate, migrate to the lymph nodes, and present TAAs to naive T lymphocytes. The third step involves the expansion of T cells in sufficient numbers to recognize and eliminate tumor cells. However, in the absence of suitable maturation signals, antigen presentation leads to T-cell anergy or generation of regulatory T cells (T_{reg}) that suppress effector T cells. Finally, antigen-educated T cells must leave the lymph node, traffic to infiltrate the tumor and persist for long enough to kill the malignant cells (Mellman et al., 2011).

Cancer vaccines can be classified as preventive or therapeutic. Preventive vaccines are administered to healthy subjects before tumor occurrence. They specifically aim to prime the host immune system, eventually eliciting long-term memory responses. Optimal results in cancer prevention were achieved with vaccine against hepatitis B virus (HBV), which prevents liver carcinomas in patients chronically infected by the virus (Finn, 2003). Moreover, The U.S. Food and Drug Administration (FDA) has approved two preventive vaccines for human papilloma virus Gardasil (HPV16) and Cervarix (HPV18), that protect against infection by the two types of HPV that cause approximately 70% of all cases of cervical cancer in worldwide (Doorbar, 2006).

On the other hand, therapeutic cancer vaccines are designed to eradicate cancer cells at late stage disease by boosting patient'own immune responses (Lollini et al., 2006). Therapeutic cancer vaccines, which have been used in many clinical trials approved by FDA, encompass different mechanisms. Some examples include the following: i) the use of antigen-presenting cells (APCs) derived from patient peripheral blood, incubated with recombinant fusion protein protein, consisting of prostatic acid phosphatase (PAP) linked with growth factors as granulocyte macrophage colony stimulating factor (GM-CSF) and infused back into the patient (Kantoff et al., 2010a); ii) recombinant viral vectors (PROSTVAC®-VF) (Kantoff et al., 2010b); iii) long-peptides for human papillomavirus and peptides in combination with immunostimulatory agents as GM-CSF (Hiltonol™ for breast cancer) (Mittendorf et al., 2012). These studies shown increase effectiveness in prolong survival patients with combinatorial

approaches; they also underline the need to establish the right quantities of antigens, the appropriate activation signals and delivery vehicles. Finally, cancer vaccines must break tolerance to reactive antitumor immune cells, highlighting the need of developing effective strategies for overcoming tumor-associated immunosuppression.
In addition to the aforementioned vaccines, there are many clinical trials financially supported by National Cancer Institute, which are available at this link: http://www.cancer.gov/about-cancer/treatment/clinical-trials/search.

1.2 Adoptive cell therapy (ACT)

The adoptive cell therapy (ACT) is a promising approach for cancer treatment in which antitumor T cells are isolated from patients, manipulated *ex vivo* and finally re-infused into the patient. The technique harnesses the power of the immune system by activating host's own T cells, which recognize and attack foreign invaders and diseased cells (Humphries, 2013). During their life, T cells move throughout tissues, scanning for MHC–peptide complexes that specifically activate their T cell receptors (TCRs). Tumor-specific T cells are activated through encounters with tumor-associated antigens that are presented by specialized APCs, including dendritic cells (DCs), which process antigens and present them to T cells in the context of MHC class II molecules or in the context of MHC class I molecules trough a mechanism known as cross-priming. Theoretically, activated T cells are capable of directly recognizing antigens that are presented on the surface of many types of tumor cells in the context of MHC class I (either naturally or as a result of gene engineering) (DuPage et al., 2012; Restifo et al., 1993; Schreiber et al., 2011). However, neoplastic cells are notoriously unstable targets, which often downregulate the expression of MHC class I molecules. Notably, one of the major limitations of ACT is the lacking of TAA recognition from T cells infused on patients (Restifo et al., 2012). Additionally, an important factor limiting the successful use of ACT in humans is the identification of cells that can recognize antigens selectively expressed on cancer cells and not on non-malignant tissues (Rosenberg and Restifo, 2015)
ACT encompasses different strategies based on either natural host cells that exhibit antitumor reactivity, or host cells that have been genetically engineered with antitumor T cell receptors (TCRs) or chimeric antigen receptors (CARs). Essentially, the ACT protocol consists in the isolation of tumor infiltrating lymphocyte (TIL), primed to attack tumor; and cultured *in vitro* with the T cell growth factor interleukin 2 (IL-2). Finally cells are infused back to the patients in association with IL-2 administration. Before to the adoptive transfer, hosts can be immunodepleted from endogenous immune system trough chemotherapy alone or in combination with total-body irradiation ensuring the cytotoxic activity of transferred T cells (Restifo et al., 2012). This strategy, dating back to 80's, (Rosenberg et al., 1986) has been improved over the past years and today it represents the best available treatment for patients with metastatic melanoma (Besser et al., 2010; Dudley et al., 2005). However, TILs therapy is still limited to patients with good performance status who are capable of withstanding the rigors of the lymphodepletion and IL-2-based treatments that are currently used. A recent study of 93 patients with stage IV melanoma described three sequential trials in which patients were treated with the adoptive transfer of autologous TILs, administered in conjunction with IL-2 following host conditioning regimens. Objective clinical response rates ranged from 49% to 72% assessed using

response evaluation criteria in solid tumors (RECIST). Although patients can sometimes benefit enormously from partial responses, every patient aspires to become cancer free. Importantly, 20 of the 93 patients (22%) achieved complete tumor regression, and 19 of these 20 (93%) have ongoing complete regression with a minimum follow up of 57 months (Rosenberg et al., 2011). Indeed, some of these patients have been alive and disease free for more than 8 years and are probably 'cured' of metastatic melanoma. The likelihood of achieving a complete response was similar regardless of prior therapy. Thus, ACT therapy with autologous TILs can mediate durable complete responses in patients with metastatic melanoma and has similar efficacy irrespective of prior treatment (Besser et al., 2010; Itzhaki et al., 2011; Rosenberg et al., 2011).

Despite these successes, the reasons why some patients respond favorably to this treatment and others do not remain unknown. At present, some studies in mice and humans have explored different aspects as the target specificities of the transferred T cells, the nature of the surrounding microenvironment and how it can be targeted (including the use of increased-intensity lymphodepletion), and finally the differentiation states of the cells involved (Restifo et al., 2012).

Scientists are working to optimize two different ACT approaches based on T cell receptor modification, one called T cell receptor (TCR) therapy and the other, more flexible, chimeric antigen receptor therapy (CAR) (Essand and Loskog, 2013). The TCR therapy consists in generation of alternative T cell receptors using viral vectors for delivery of genes encoding the new TCR. T cells after TCR engineering could recognize specific tumor antigens and they can also express factors that allow their persistence in the body. This method showed good results in clinical trials for metastatic melanoma, colorectal cancer and synovial cancer (Robbins et al., 2011). Despite the promising results, the use of TCR therapy is limited by the need of genetically match of the new receptor with patients' immune type. CAR therapy seems more adaptable for avoiding this constraint, using a gene that encodes artificial, antibody-like proteins that bind the antigens on the tumor cell's surface without needing to match the patient's immune type. CARs are composed of three pieces: an antibody that binds to a common cancer antigen; part of a receptor that activates the cell; and one or more stimulatory molecules that help the T cell proliferate and persist. CARs after their insertion and expression on T cell, work as a switch, in fact when they matched with tumor antigen, immediately activate T cell into attack mode. Although the potential of CAR, their use is reported only in small clinical trials, where it was reported good results on treatment of B-cell leukaemias and lymphomas, focusing on CD19 protein expression (Kochenderfer et al., 2010). Although the positive results derived from clinical trials of ACT, this field still needs to be improved before a massive use in clinical. First, it is necessary the development of specialized cell production facilities and staff trained in genetically modifying and growing the cells. Moreover, it is fundamental to modulate the strength of immune cells to direct the cytotoxic attack only to neoplastic cells avoiding normal tissues, which can express similar antigens. Until now it is not totally understood why only some patients take benefits of ACT.

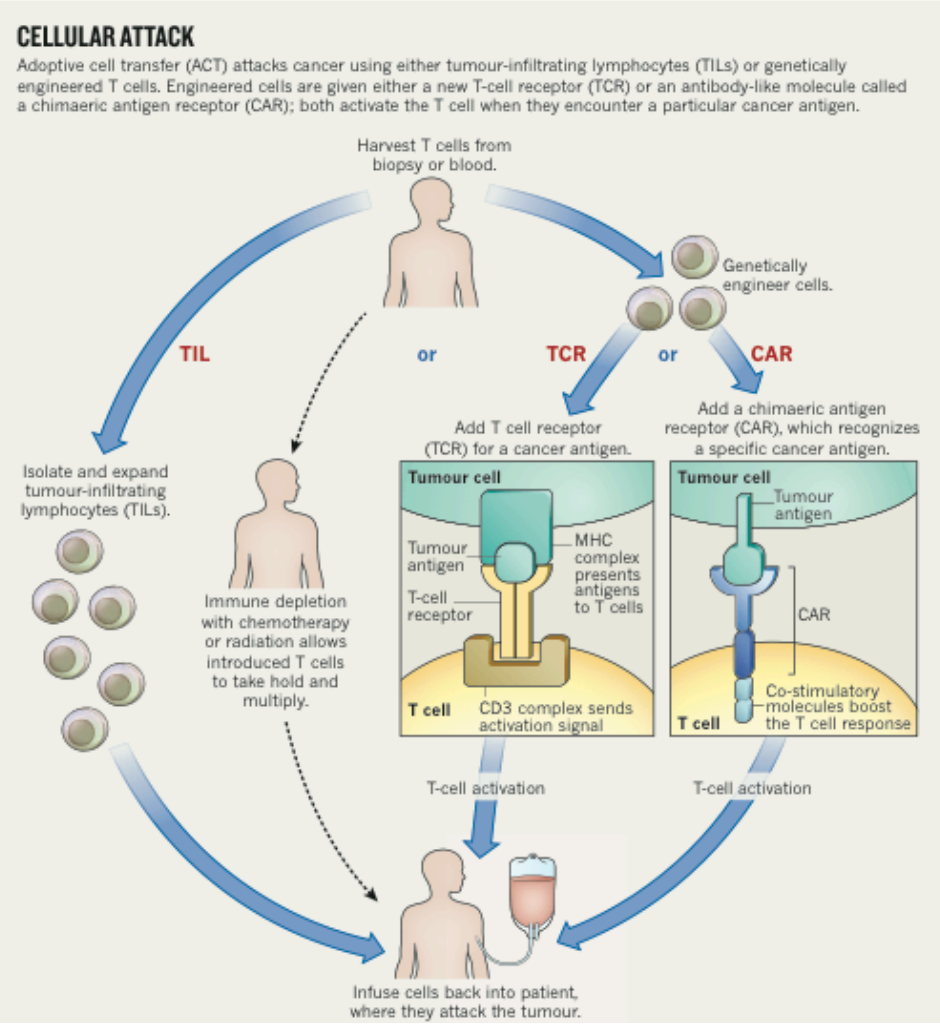

Figure 1. Schematic representation of different types of adoptive cell transfer. TILs re-infusion (left); (centre) TCR therapy; (right) CAR therapy (Humphries, 2013)

2. Tumor microenvironment complexity

In the last decade it became clearly that tumor mass is a complex structure composed not only by neoplastic cells, but also from different cell populations which sustain cancer growth. Tumor microenvironment emerges from a complex framework where different corrupted resident or purposely recruited cells exert conflicting functions establishing a peculiar cytokine milieu. The stromal components of tumor microenvironment can be classified into three general classes: angiogenic vascular cells, cancer-associated fibroblastic cells and infiltrating immune cells (Hanahan and Weinberg, 2011). Remarkably, the localization, the type and numbers of immune cells infiltrating tumors correlate with patterns and subsets of prognostic biomarkers, first observed in colorectal cancer (Nosho et al., 2010; Ogino et al., 2009) and later introduced in clinical as novel parameter, called "immunoscore". This new index supports cancer staging and identifies patients with high-risk of tumor recurrence, also facilitate clinical decisions as the rational stratification of patients could have major benefit from adjuvant therapy. The "immunoscore" considering the immune cell density, calculated by numerical quantification of two lymphocyte populations, cytotoxic and memory T cells both at the tumor core and the invasive margin (Galon et al., 2012).

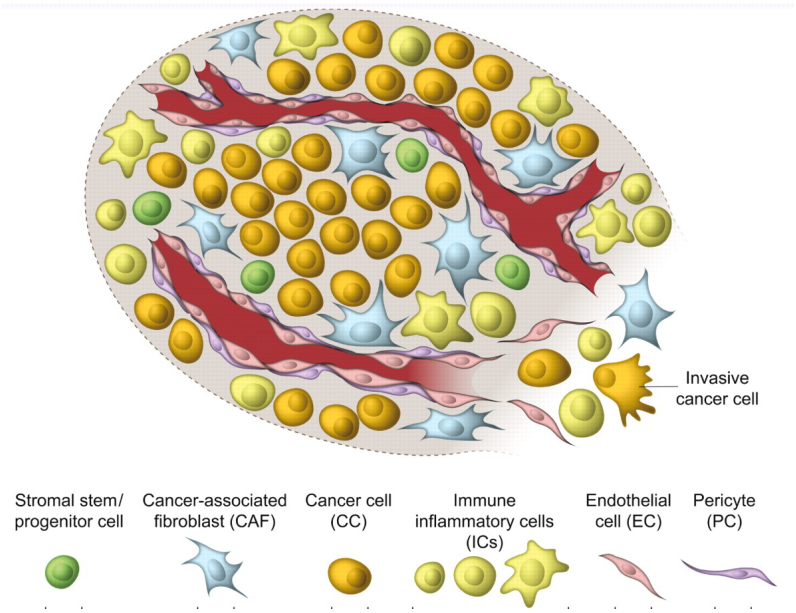

Figure 2. Tumor heterogeneity. The tumor microenviroment is composed by cancer cells interacting dynamically with immune inflammatory cells, endothelial cells, fibroblast cells and endothelial cells (Sherman et al., 2012)

Vascular endothelial cells and their associated pericytes, are fundamental during neovascularization, in fact those cells can originate new vessel from existing ones after sensing of soluble factors as vascular endothelial growth factors (VEGFs), fibroblasts growth factors (FGFs), platelet-derived growth factors (PDGFs) and chemokines produced from malignant cells and also from inflammatory cells (Carmeliet and Jain, 2011). The new vessels create chaotic vasculature in the tumors, which is characterized by leakiness of the raises, which cause unevenness of blood flow, oxygenation, nutrients and drug distribution in the tumor microenviroment. These anarchic structure, increases hypoxia and facilitate

metastasis (Jain, 2005). Cancer associated fibroblasts (CAFs), are myofibroblasts differentiated from some precursors such as smooth muscle cells, myoepithelial cells, mesemchymal cells and endothelial cells. (Brittan et al., 2002; Spaeth et al., 2009; Tomasek et al., 2002; Willis et al., 2006). CAFs, differently from normal fibroblasts, which typically suppress tumor formation show pro-tumorigenic properties, since they enhance tissue remodeling, by increasing expression of proteolytic enzymes, such as matrix metalloproteinases, and extracellular matrix deposition. Moreover CAFs secrete distinctive factors as the stromal cell-derived factor 1 (SDF1), VEGFs, PDGFs, and the hepatocyte growth factor (HGF), promoting immune cell recruitment at tumor site (Polanska and Orimo, 2013). Distinct immune cell subsets so far populate the crowded tumor environment. Tumor-infiltrating immune cells comprise cells belonging to both subsets the adaptive and the innate immune compartments. Obviously, numerous cytotoxic lymphocytes $CD8^+$ T cells and helper $CD4^+$ T cells infiltrate the tumor microenvironment at the invasive margin and the lymphoid organs, normally their presence is associated with good prognosis. Over T lymphocytes, it was also reported the presence of natural killer (NK) cells, γδ T cells and natural killer T cells (NKT) and segregated B cells organized as tertiary lymphoid structures (TLS) (Goc et al., 2014). The role of these structure also the innate lymphocytes still not clear in the tumor microenvironment, it seems their activity could switch from anti-tumor to pro-tumor depending con the cytokines released in the milieu (Gajewski et al., 2013). Furthermore, myeloid population infiltrating tumor microenvironment, with mostly pro-tumor activity, encompass both terminally differentiated cells, as DCs, macrophages and granulocytes, and immature myeloid cells, as MDSCs, which are generated from bone marrow as a consequence of a cancer-induced abnormal myelopoesis (Gabrilovich et al., 2012). As anticipate above, DCs recruited within tumor microenvironment favor tumor evasion as consequent of the down-regulated expression of the MHC class II and co-stimulatory molecules CD80 and CD86, they do not adequately stimulate an effective immune response against tumor cells (Gabrilovich, 2004). Macrophages in the tumor core, called tumor associated macrophages (TAMs), exhibit M2 phenotype, or alternatively activated macrophages, which is activated by IL-4, IL-10, IL-13 and glucorticoid hormones, are characterized by secretion of high levels of IL-10 and low levels of IL-12 and favoring tumor progression (Mantovani et al., 2002). In fact, TAMs, on the contrary of M1 or classically activated macrophages with tumoricidal activity, shown poor antigen presenting capacity, promote angiogenesis and lymphangiogenesis, sustain tissue remodeling, tumor invasion and metastasis, and suppress anti-tumoral adaptive immunity. The same picture for the tumor associated granulocytes, which are mostly neutrophils, which shift from anti-tumor N1, characterized by high expression of immunoactivating cytokines and chemokines, to pro-tumoral phenotype N2 following TGF-β exposure, which is frequently secreted by cancer cells (Fridlender et al., 2009).

Finally, MDSCs, heterogeneous population that include direct progenitors of DCs, macrophages and granulocytes and exploit multiple redundant mechanisms to influence both innate and adaptive immune responses, which can be grouped in four classes. The first, MDSCs induce the activation and expansion of regulatory T cells (T_{reg}) population by promoting antigen-specific natural Treg clonal expansion and naive $CD4^+$ T cell conversion into induced Treg cells. The second is based on nutrients depletion required by lymphocytes, i.e. L-cysteine

sequestration and L-arginine depletion through arginase1 (ARG1) dependent consumption, which cause TCR ζ-chain down-regulation and the proliferative arrest of antigen-activated T cells. The third interfering with lymphocyte trafficking and viability, by expressing at the plasma membrane ADAM17 (disintegrin and metalloproteinase domain-containing protein 17), which cleaves key proteins for T cell recirculation to lymph nodes, and galectin-9 (GAL-9), which induce T cell apoptosis. Finally, the fourth sustain oxidative stress within production of reactive oxygen species (ROS), nitric oxide (NO) and other reactive nitrogen species (RNS), by the synergistic activity of ARG1, iNOS and NADPH oxydase enzymes in the tumor microenvironment (Gabrilovich et al., 2012).

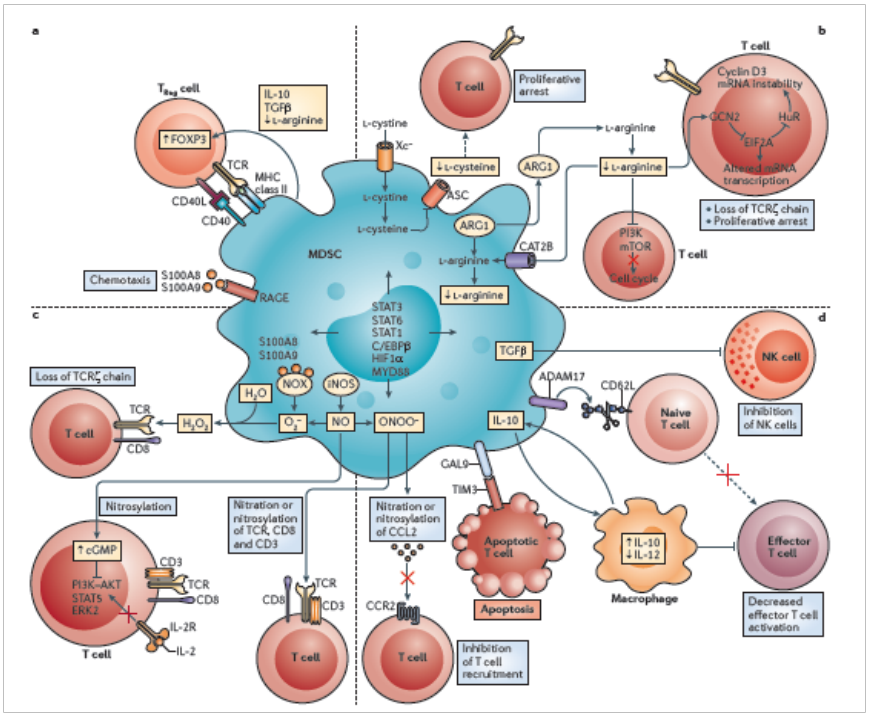

Figure 3. Mechanisms of MDSC-dependent inhibition of T cell activation and proliferation. Myeloid-derived suppressor cells (MDSCs) can inhibit efficient antitumour T cell responses through a number of mechanisms. a) Tumour-associated MDSCs induce the development of regulatory T (T_{reg}) cells or expand existing T_{reg} cell populations. b) Tumour-associated myeloid cells deprive T cells of amino acids that are essential for their growth and differentiation. c) Tumour-associated myeloid cells release oxidizing molecules, such as hydrogen peroxide (H_2O_2) and peroxynitrite (ONOO–) which cause nitration and nitrosylation of components of the T cell receptor (TCR) signalling complex, and the loss of the TCR ζ-chain, thereby inhibiting T cell activation through the TCR. d) Tumour-associated myeloid cells can also interfere with T cell migration and viability through ADAM17 and GAL9 expression.

3. Nitric oxide production in biological systems

NO is a stable colorless gas under atmospheric condition, which freely crosses cell membranes, blood and tissues with solubility and diffusion similar to oxygen; those characteristics are ascribed to the size (30 Da) and the absence of charge (Alderton et al., 2001). NO is involved in many different physiological and pathological conditions depending on its synthesis and concentration (Moncada et al., 1991). In biological systems, NO is generated enzymatically from L-arginine by NO synthase enzymes (NOS), according to the following chemical reaction:

$$\text{Arginine} \xrightarrow[O_2 \rightarrow H_2O]{NADPH + H^+ \rightarrow NADP^+} \text{N-Hydroxyarginine}$$

$$\xrightarrow[O_2 \rightarrow H_2O + NO]{½\ NADPH + H^+ \rightarrow ½\ NADP^+} \text{Citrulline}$$

This reaction is catalysed by three different types of NOS enzymes, with 51-57% homology between the human isoforms, suggesting the existence of a common ancestral NOS gene: neural (nNOS or NOS1), inducible (iNOS or NOS2) and endothelial (eNOS or NOS3). NOS enzymes have similar genomic organization although, they are encoded by different genes with different localization, regulation, catalytic properties and inhibitor sensitivity. The nNOS gene is localized in a single position on human chromosome 12 and containing an intron gene at least of 20 kb (Hall et al., 1994). The eNOS gene is located on chromosome 7 whereas the iNOS gene is mapped to chromosome 17 (Janssens et al., 1992). Although different locations on human chromosomes, the NOS enzymes show similar structure composed by bidomains: an NH_2-terminal catalytic oxygenase domain that binds heme (i) iron protoporphyrin IX), tetrahydrobiopterin (BH_4), and the substratel-Arg; (ii) a COOH-terminal reductase domain that binds flavin mononucleotide (FMN), flavin adenine dinucleotide (FAD), and NADPH; and (iii) an intervening calmodulin-binding region (Habib and Ali, 2011). Calmodulin increases the rate of electron transfer from NADPH to the reductase domain and triggers electron transfer from the reductase domain to the haeme centre (Matsuda and Iyanagi, 1999); it also is involved in the formation of a homodimer, followed by intracellular Ca^{2+} variation, resulting in enzyme activation. Calcium acts as a modulator especially for NOS1 and NOS3, which require higher amount for their activity than NOS2 (Tengan et al., 2012)

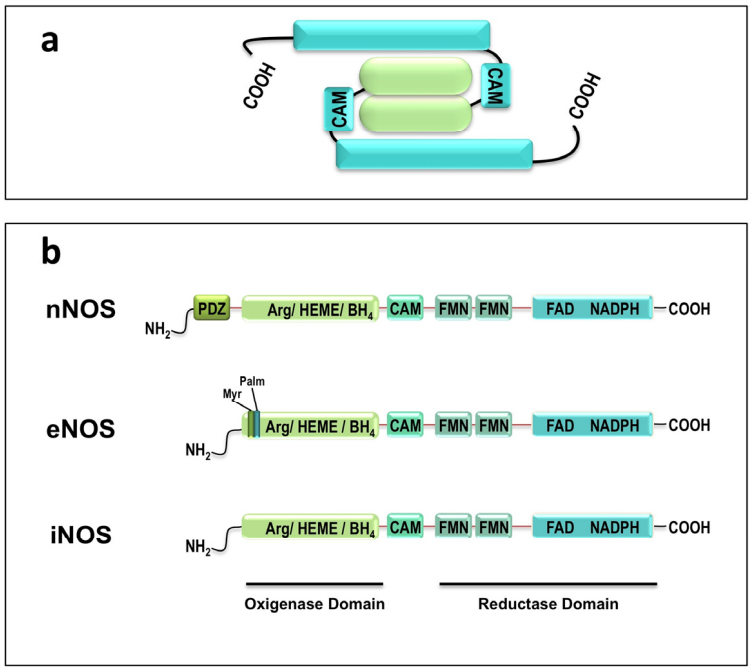

Figure 4. Schematic diagram illustrating domains and structure of human NOS enzymes. (a) Schematic representation of the diametric conformation of nitric oxide synthases (NOS) with both subunits attached at the oxygenase domains (green); (b) Domains structures of differences of three isoforms nNOS, eNOS and iNOS of NOS isoforms. PDZ domain is typically present in neuronal NOS (nNOS), the presence of myristoylation (Myr) and palmitoylation (Palm) sites are specific to endothelial NOS (eNOS). All isoforms the oxygenase domain contains binding sites for l-arginine (Arg), Heme and tetrahydrobiopterin (BH4), calmodulin (CAM), the reductase domain binds FMN, FAD and NADPH (Tengan et al., 2012).

nNOS and eNOS, also referred as constitutive NOS (cNOS), are constitutively expressed among several cell types, including the vascular endothelium cells, platelets, and neurons. The cNOS in response to physiological stimuli that trigger intracellular Ca^{2+} rise produce low levels of NO rapidly and transiently. Low-levels of NO produce rapid transient cellular response as like modulate neural activity, blood flow, smooth-muscle relaxation. On the contrary the inducible NOS is not express on resting cells but it is induced by immunologic and inflammatory stimuli such as endotoxin (lipopolysaccharide, LPS) or cytokines as interferon gamma (INF-γ), interleukin-1 (IL-1) and tumor necrosis factor alpha (TNF-α) (Alderton et al., 2001). After a lag period necessary for protein synthesis iNOS produce high amount of NO, which acts directly with cytotoxic effect against pathogens as like *Mycobacterium*, *Listeria monocytogenes* and *Leishmania maijor*. Finally, recent studies reported another enzyme as NO producer, named mithocondrial NO synthase (mtNOS). This enzyme activity calcium dependent is fundamental to mitochondria homeostasis, was described firstly at rat liver, where it is constituvely active (Ghafourifar and Cadenas, 2005).

3.1 Nitric Oxide direct biological effects: focus on immune system

Nitric oxide, at low concentration as omnipresent intercellular messenger, regulates many physiological processes as blood flow (Wolin, 2009), and neurotransmission (Steinert et al., 2011). These functions are classified as direct effects of NO, which is mainly produced by the cNOS enzymes (NOS1 and

NOS3) associated with the intracellular calcium concentration. In addition, NO plays fundamental role in immune system especially for antiviral and antimicrobial activities, both cytotoxic (tissue-damaging) and cytoprotective (tissue-preserving), acting as either an immune-stimulatory (pro-inflammatory) or immunosuppressive (anti-inflammatory) agent (Predonzani et al., 2015). Most of NO production in immune cells derived from iNOS enzyme activity in macrophages or other host cells, which also provokes the depletion of local arginine (together with ARG1) sustaining growth inhibition and death of the parasites.

Since NO activity depends on its local spatio-temporal concentration, the phenotype and functional commitment of the immune cells, responsible for its generation, dramatically impact on its own activity. Generally, macrophages after cytokines or microbial stimulation, sustain cytostatic or cytotoxic activity, through iNOS expression, against pathogens and tumor cells (Farias-Eisner et al., 1994; MacMicking et al., 1997). Historically, macrophages were classified into two major categories (M1/M2) depending on their activation status and inflammatory attitude. Once differentiated, M1 or classically activated macrophages trigger Th1 immune response and secrete high amounts of NO to kill intracellular pathogens and to exert cytotoxicity towards tumor cells (Sica and Mantovani, 2012). On the other side, M2 macrophages express high levels of ARG1, which competes with iNOS for their common substrate L-arginine, thus preventing NO generation. This paradigm underlines that NO represents a remarkable hallmark of macrophages activation in pathological settings as infection or cancer, where they may exert divergent roles (Biswas and Mantovani, 2010; Murray et al., 2014). Considering macrophages plasticity, it has been proposed that in the early stages of tumor progression, macrophages exploit high concentrations of NO and RNS to kill tumor cell clones. Later on, macrophages corrupted by tumor microenvironment produce low levels of NO/RNS, which in turn promote cancer growth and spreading. The dichotomous activity of macrophage-derived NO definitely mirrors their functional plasticity in response to environmental cues. The multifaceted role of NO in cancer biology will be discuss below in the proper paragraph of this text named “The intricate role of nitric oxide in cancer biology.”

Beyond macrophages, there are alternatives sources of NO in immune system (Coleman, 2001).

Interestingly, recent works described a new subset of dendritic cells, able to produce nitric oxide trough iNOS expression, named TNF/iNOS (Tip) producing dendritic cells (Tip-DCs). Until these recent reports the role of DCs as potential NO-producing cells were debated and so far it has not been fully investigated the expression of iNOS as well as NO production participate in the innate defence against intracellular pathogens (Serbina et al., 2003).

3.2 TNF/iNOS producing dendritic cells: new source of nitric oxide.

Inflammatory immune responses against tumors and invading pathogens require the recruitment of immune cells to the site of damages. In this context, a key role is played by DCs, which are considered the most powerful antigen presenting cells, representing the bridge between innate and adaptive immunity (Katsnelson, 2006). In the canonical maturation pathway, microbial products trigger DC activation, which leads to the production of large amounts of cytokines, especially interleukin-12 (IL-12) and IFN-α, driving the differentiation of naive T-cells into

effector cells (Smith-Garvin et al., 2009). Moreover, DCs exposed to inflammatory cytokines rapidly activate other innate protective cells such as NK and NKT cells (Fernandez et al., 1999).
Based on distinct surface markers **(Table 1)**, DCs are phenotypically divided in different cell subpopulations: i) conventional DCs (cDCs) derived from common DC progenitors (CDP) which are divided in two main categories migratory DCs and lymphoid tissue-resident DCs; ii) alternatively DC differentiated from monocyte intermediate precursors and finally iii) non-conventional plasmacytoid DCs (pDCs) (Belz and Nutt, 2012).

DC subset	DC type	CD8α	CD103	CD205	EPCAM (CD326)	CD11b	B220 or CD45RA	DC-SIGN	Langerin (CD207)	Antigen presentation	Major cytokine produced
pDCs	Lymphoid-resident DCs	+/–	–	–	–	–	+	++	–	Poor	IFNα
CD8α⁺ DCs	Lymphoid-resident DCs	+	low	+	–	+	–	–	+/–	Cross-presentation on MHC class I; expression of cystatin C	IL-12p70, IFNλ
CD4⁺ DCs	Lymphoid-resident DCs	–	–	–	–	+	–	–	–	Presentation on MHC class II	
DN DCs	Lymphoid-resident DCs	–	–	–	–	+	–	–	–	Presentation on MHC class II	
CD11b⁺ DCs	Migratory DCs	–	+/–	+	–	+	–	ND	–	Presentation on MHC class II	
CD103⁺ DCs • Lung • Intestine	Migratory DCs	– –	+ +	++ –	+/– –	– +	– –	– –	+ –	Cross-presentation on MHC class I	
Langerhans cells	Migratory DCs	–	–	++	+	+	–	–	++	Presentation of self antigens for tolerance induction	IL-10
Monocyte-derived DCs	Induced by inflammation	–	–	–	–	+	–	+	–	Cross-presentation	TNF

DC, dendritic cell; DC-SIGN, DC-specific ICAM3-grabbing non-integrin; DN, double-negative; EPCAM, epithelial cell adhesion molecule; IFN, interferon; IL, interleukin; ND, not determined; pDC, plasmacytoid DC.

Table 1. Phenotypic markers of DCs.

Recently, as anticipate above, Serbina and colleagues described a novel subset of dendritic cells, Tip-DCs. In this work performed with a mouse models of *L. monocytogenes* infections, it was observed a population defined by these surface markers as $CD11b^{int}$ $CD11c^{int}$ $Gr\text{-}1^{+}$ $DEC\text{-}205^{-}$ $CD14^{-}$ $F4/80^{-}$ associated with morphology like-DC and also no adherence. Additionally to the co-stimulatory markers, these cells resulted able to prime T cells and also to produce NO and TNF-α. These features forge the name as TNF/iNOS producing dendritic cells. In this study, the authors described the antimicrobial activity of Tip-DCs, which were recruited in the infection site by the CCR2-signalling. Moreover, Tip-DCs ($CD11b^{+}Ly6C^{+}CD11c^{+}$) were also described in *Trypanosoma brucei* infection model, where they exerted cytotoxic effects in the liver during the infection (Bosschaerts et al., 2010). In this model, $CCR2^{+}$ inflammatory monocytic cells, derived from CD11b and Ly6C expressing cells, were described as probably precursor of liver Tip-DCs. In this experimental model, the differentiation to Tip-DCs from immature DCs ($CD11c^{+}$ but CD80/CD86/MHC-class II^{low}) is independent of IFN-γ and MyD88 signaling, whereas IFN-γ stimulation is necessary for TNF and iNOS/NO production (Bosschaerts et al., 2010).
Based on the facts mentioned above, it is reasonable to conclude that Tip-DCs may derive from $CCR2^{+}$ $Ly6C^{high}$ (Serbina and Pamer, 2006) macrophage/DC

progenitor (MDP) cells and have the potential to produce TNF/NO after appropriate stimulation (Schmid et al., 2012). Moreover it is also known that bone marrow-derived DCs ($CD11c^+$, $CD11b^+$, $F4/80^-$) are able to produce TNFα and iNOS after stimulation (Ritter et al., 2003; Munder et al., 1999). Thus, it is difficult to see the dissimilarity between TiP-DCs and other activated monocyte-derived cells (Taylor et al., 2005; Hume, 2008). In other words, it cannot be excluded that Tip-DCs do not represent a distinct DC subset but rather belong to common monocyte-derived DC responding to their environment with TNF/NO production (Serbina et al., 2003). In addition to evidences from murine models, Tip-DC were described also in humans but in this first study their origin is ascribed to blood-monocytes (Chong et al., 2011). Indeed, it is clear that additional studies are required to further characterize these cells their mechanisms of recruitment, functions and origins.

3.3 The CD40/CD40L axis.

DCs interact with T lymphocytes trough the major histocompatibility complex (MHC) proteins expressed on their surface, and co-stimulatory receptors as CD40. CD40 is a transmembrane glycoprotein surface receptor that is a member of the Tumor Necrosis Factor Receptor superfamily (TNFRSF), originally described on B cells. (Caux et al., 1994; Pinchuk et al., 1994). Cd40 signalling plays a key role in DC maturation and activity; in particular it promotes the upregulation of MHC class II and co-stimulatory molecules CD80/CD86, thus making DCs more effective APCs(Caux et al., 1994; Sallusto and Lanzavecchia, 1994). The ligand for CD40, CD154 (also known as TRAP, T-BAM, CD40 Ligand or CD40L) is a integral type II membrane protein. Initially, CD40L was reported to be expressed principally on activated $CD4^+$ T cells, thus providing T cell help to B cells (Banchereau et al., 1994). Additionally, CD40L expression on activated T cells provides co-stimulation for effector T cell functions (van Essen et al., 1995; Grewal et al., 1995) as well as it mediates proper 'licensing' of DCs and APCs to prime $CD8^+$ T cells. (Kelleher and Beverley, 2001). Behind the initial classification,, it has been reported that CD40 molecules is also expressed on bone marrow stroma or tumor stromal cells (Beatty et al., 2011; Ma and Clark, 2009). CD40L is expressed primarily by activated T cells, as well as activated B cells and DCs but it can also be induced on monocytes, NK cells, mast cells, and basophils under inflammatory conditions (Ma and Clark, 2009). An interesting aspect to be considered is the CD40-CD40L-dependent bidirectional crosstalk that occurs between DCs and lymphocytes. Indeed, it was shown that CD40-CD40L interactions between T cell and DCs provides reciprocal effects that both regulate T cells and DCs (van Essen et al., 1995). While it is clear that CD40L crosslinking can signal T cells e.g., to produce IFN-γ (Grewal et al., 1996; Mackey et al., 1998), it is not clear how ligation of CD40L on B cells or DCs affects their functions.

The CD40-CD40L axis plays a prominent role in tumor biology. Indeed, although normally induced by helper T cells, CD40 signaling on APCs can also be effectively triggered using agonistic antibodies or CD40L (Khong et al., 2012). This represents the rationale for CD40 agonist-based cancer immunotherapy. CD40 has been exploited as a target for the treatment of different cancers using either recombinant soluble CD40L (sCD40L) or agonistic therapeutic antibodies

(Abs) (Khong et al., 2012). CD40 mAb represent so far a new therapeutic option in cancer, which has the potential to generate anticancer immunity by various mechanisms. In an elegant study, it has been recently demonstrated that CD40 agonists are able to induce T cell-dependent and independent tumor regression in patients with pancreatic cancer (Beatty et al., 2011).

3.4 The intricate role of nitric oxide in cancer biology

As mentioned before, NO plays multiple role in cancer biology. Mostly of the NO effects in cancer are indirect actions caused by NO metabolites (Pacher et al., 2007). Specifically, NO in cancer may act as tumor promoter or inhibitor depending on several factors as: NOS isoforms expression, source of NO production, concentration and timing of NO exposure and finally the sensitivity of cells to this radical (Fukumura et al., 2006).

At the tumor site, NO combines with other radicals, leading to RNS generation that sustains genomic instability and blocks antitumor immune responses.

Basically, high concentrations of NO and RNS can arrest cell cycle or induce cell death, whereas low concentrations may protect cells from apoptosis. High levels of NO/RNS post-translationally modify death-related target proteins, as the death receptors of the TNFα superfamily (Leon et al., 2008). Moreover, high NO concentrations, oxidizing and/or deaminating the DNA bases, result in DNA breaks, DNA base modifications or DNA cross-links, which cause mutations that may either activate oncogenes or deactivate tumor suppressor genes. In addition, NO/RNS-driven protein modifications such as S-nitrosylation or nitration may inhibit proteins belonging to the DNA repair systems, driving to genomic instability

Low concentration of NO sustains angiogenesis and metastasis. NO orchestrates angiogenesis, by maintaining the blood flow and vessel dilation during cancer development. NO also induces vascular endothelial cell proliferation and migration trough the release of VEGFs which are fundamental for metastasis (Franchi et al., 2006; Fukumura et al., 2006). NO may also inhibit the aggregation of platelets through a cGMP-dependent mechanism, preventing aggregates formation with tumour cells, which may facilitate their adhesion to vascular endothelial cells and haematogeneous dissemination (Ogino et al., 2009).

As previously mentioned, NO/RNS can suppress tumour-specific adaptive immunity through several mechanisms. The suppression of antitumor immune activity within the tumor microenvironment is induced in several ways. One is the arrest of adaptive immunity, induced either by inhibition of phosphorylation, or the activation of important signaling proteins in the IL-2-receptor pathway including Janus activated kinase 1 (JAK1), JAK3, STAT5, extracellular-signal-regulated kinase (ERK) and AKT in T cells (Bingisser et al., 1998). Another mechanism of NO/RNS immunosuppression is the post-translational modifications of key proteins for T cell activation such as CD8 and TCR complex α/β chains molecules (Nagaraj et al., 2007), and the impairment of T lymphocyte recruitment to the tumor site, due to the posttranslational modification of the CCL2 chemokine (Molon et al., 2011).

On the other hand, NO plays also antitumor activity mostly exerted directly by high levels of NO, which can be summarized as cell cycle arrest (cytostatic effect) and cell death induction. The cytostatic effect based on the production of high levels of NO, and consequent RNS is the major weapon in the

macrophage's arsenal against pathogens and tumor cells (Weigert and Brüne, 2008). In addition, NO may induce apoptosis either via downregulation of the anti apoptotic protein survivin, as observed in human lung carcinoma cells (Chao et al., 2004), or upregulation of Fas expression, as shown in ovarian carcinoma cell lines, through the specific inactivation of the transcription repressor yin-yang-1, which binds to the silencer region of the Fas promoter (Bonavida, 2010).
Finally, another way to induce apoptosis is the post-translational modification induced by high levels of NO/RNS of death-related target proteins, as the death receptors of the TNFα superfamily, and block respiration in target cells by affecting the mitochondrial respiratory chain and its outer membrane permeability and thus leading to the release of cytochrome c and apoptosis initiation (Leon et al., 2008)

In addition to NO dichotomous role in tumor, some controversial evidence is also reported for NOS isoform localization, which is strictly correlated to cancer type. Certainly, NOS2 is the most expressed isoform in cancer and it is markedly expressed in approximately 60% of breast cancer, at 20% -25% respectively in colon adenomas and carcinoma. Moreover, NOS2 was also reported in other cancer types as head and neck, esophagus, lung, prostate, bladder and pancreatic carcinomas, brain tumors, Kaposi's sarcoma, mesothelioma, and hematological malignancies. (Fukumura et al., 2006) In some cases NOS2 expression in the tumor cells was inversely correlated with tumor stage, grade and progression, and positively correlated with apoptosis and patient survival (Fukumura et al., 2006).

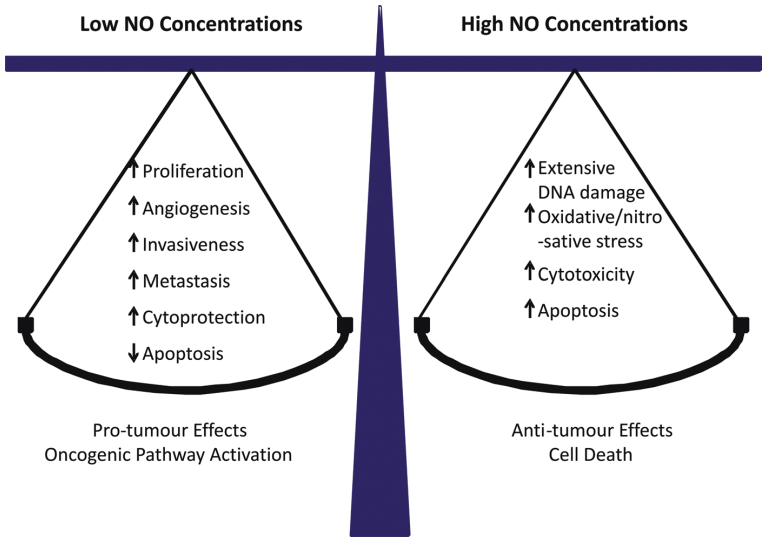

Figure 5. Mechanisms of action of NO on tumor cells. NO can induce both pro-tumor effects at low concentration promote increase proliferation and angiogenesis, medium concentrations promotes increased invasiveness, metastasis increase cytoprotection and reduce apoptosis. At high concentration, promote DNA damages, oxidative/nitrative stress, cytotoxicity and apoptosis (Burke et al., 2013).

4. Methods to detect Nitric oxide production in biological systems

Since NO is involved in many physiological and pathological conditions, the precise detection and quantification of this chemical mediator is pivotal to understand its activity in the different biological contexts. Due to the extremely short half-life of this free radical, its very low, in some cases subnanomolar, physiological concentrations and to its high reactivity toward oxygen and many other substances, NO measurement represents a technical challenge for scientists. A possible way to overcome the transient nature of NO in biological samples is to measure its stable metabolites, nitrate and nitrite. The quantification of NO metabolites in biological samples provides valuable information with regards to *in vivo* NO production, bioavailability and metabolism. Nonetheless, this approach does not provide information on instantaneous NO concentration or the rate of NO generation, which can be physiologically relevant.

Indeed, methods continue to be developed and validated allowing the detection and quantification of NO and NO-related products/metabolites in multiple compartments of experimental animals (Bryan and Grisham, 2007).

NO determination may be performed by either direct or indirect methods. Direct NO detection is based on the use of fluorimetric probes (Kojima et al., 1998) whereas indirect methods employ other approaches such as spectrophotometric measurements (Grisham et al., 1996). One spectrophotometric method is the Greiss reaction consisting of a two-step diazotization reaction in which the NO-derived nitrosating agent, dinitrogen trioxide (N2O3) generated from the acid-catalyzed formation of nitrous acid from nitrite (or autoxidation of NO) reacts with sulfanilamide to produce a diazonium ion which is then coupled to *N*-(1-napthyl) ethylenediamine to form a chromophoric azo product that absorbs strongly at 540 nm (Grisham et al., 1996). Despite these method is only an indirect determination of NO production, it is useful for the easy quantification and also for the commercial available preparation.

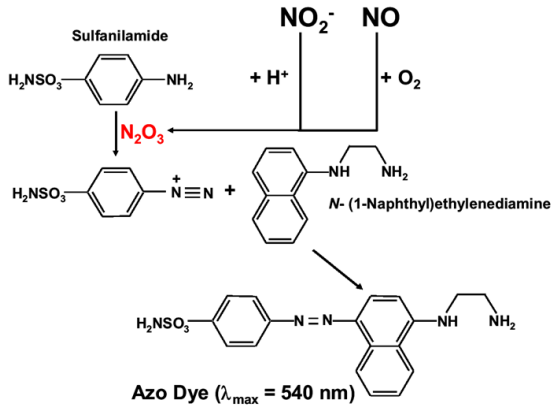

Figure 6. The Greiss reaction. The nitrosating agent dintrogen trioxide (N_2O_3) generated from acidified nitrite (or from the autoxidation of NO) reacts with sulfanilamide to yield a diazonium derivative. This reactive intermediate will interact with N-1-naphthylethelene diamine to yield a colored diazo product that absorbs strongly at 540 nm. (Bryan and Grisham, 2007)

Another spectrophotometrical assay is the High Performance Liquid Chromatography (HPLC) Determination: a dedicated HPLC system developed by EiCom Corporation allows sensitive and selective measurement of nitrite and

nitrate in all biological matrices with ease and high throughput. The high sensitivity derived from the combination of HPLC with Greiss reaction for the detection.

The fluorimetric methods, as fluorescence imaging, have many advantages in view of its sensitivity, selectivity, spatiotemporal resolution, and experimental feasibility. Thus, a variety of fluorescent probes have been developed since the 1980s. The ideal fluorescent probes for NO bioimaging should have the following characteristics: water solubility, membrane permeability, non-cytotoxic, high sensibility and sensitivity for NO and its derivatives at low levels also for its variation, finally excitable at low-energy at low-energy wavelengths so that the induced auto-fluorescence can be effectively prevented (Li and Wan, 2015). Although some fluorescent probes were designed during the last years and they can be classified in two main groups organic-based and metal-based fluorescent probe, both became widely used in NO studies (Li and Wan, 2015).

The organic-based fluorescent NO probes are mostly composed of two elements: a NO-reactive moiety and a fluorophore. The NO-reactive moiety act as a modulator in the photoinduced electron transfer (PeT) mechanism, which quenches the fluorescence of fluorophores until it binds with the NO or NO oxidized products (Hall and Garthwaite, 2009). This structure has been widely used to develop NO-responsive organic-based probes as DAF-FM and DAF-4M AM. Both probes contain o-diamine as functional groups. The electron-rich vicinal amines are thought to transfer energy to the aromatic group with PeT to quench the fluorescence. An o-diamine functionality reacts with an oxidized form of NO to produce an electron-poor fluorescent triazole derivative, which dissipates the PeT pathway and restores the fluorescence (Nagano and Yoshimura, 2002).

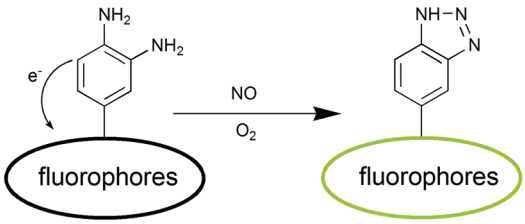

Figure 7. Mecchanism of florescence probes based on o-diamine probes. The probes until reaction with NO is colorless, while the NO- binding induce fluorescence emission.

DAF-FM is the result of an evolution of development of fluorescent o-diamine probes, in fact the first classes of fluorescent probes DAFs incorporate fluorescein with unstable fluorescence while DAF- FM was based on the increased resistance to photo-bleaching of fluorinated fluorescein derivatives. DAF-FM contains substituted fluorine atoms at the 2′ and 6′ positions and an N-methyl group, also a diacetate or acetoxymethyl ester moiety, which can be readily hydrolized by intracellular esterases, was introduced to make it membrane permeable (Kojima et al., 1998). Further the photo-bleaching DAF-FM resulted sensitive to ph variation, so the same group designed rhodamine B fluorophore-based probes named diaminorhodamines (DARs), comprising DAR- 4M AM. Similar to DAF-FM,

DAR-4M AM is the result of evolution of many probes designed earlier, anyway it structure contain one of the amines replaced with methylamine. DAR 4M AM show stable fluorescence, high sensitivity at low concentration of NO (7nM) and stability to intracellular ph variation (Itoh et al., 2000).

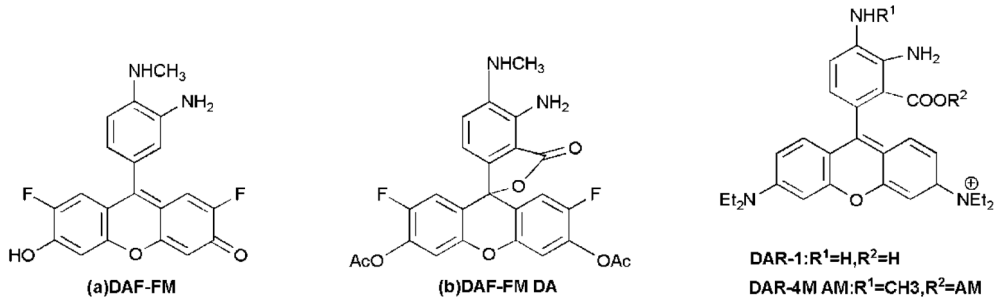

Figure 8. Structures of o-diamine probes. Diamminofluoresceins probes from in (a) chemical structure of DAF-FM, in (b) DAF-FM DA, in (c) chemical structures of diamminorhodamine probes.

Since both probes as DAF-FM as DAR-4M AM are commercially it is reported from several works their application to detect NO in biological experiments as the production in macrophages or in endothelial cells.

Finally, the metal- transition based fluorescent probes, which structure contains a fluorescein modified with an appended metal-chelating ligand, the incorporated fluorophore can be quenched by intracellular photoinduced electron transfer and/ or coordination to a paramagnetic or heavy metal ion. These probes can form direct and reversible bond with nitric oxide, becoming the best choice for the detection in real time of NO production, while others probes recognize the oxidized form and establish irreversible bonds with NO (Lim, 2007).

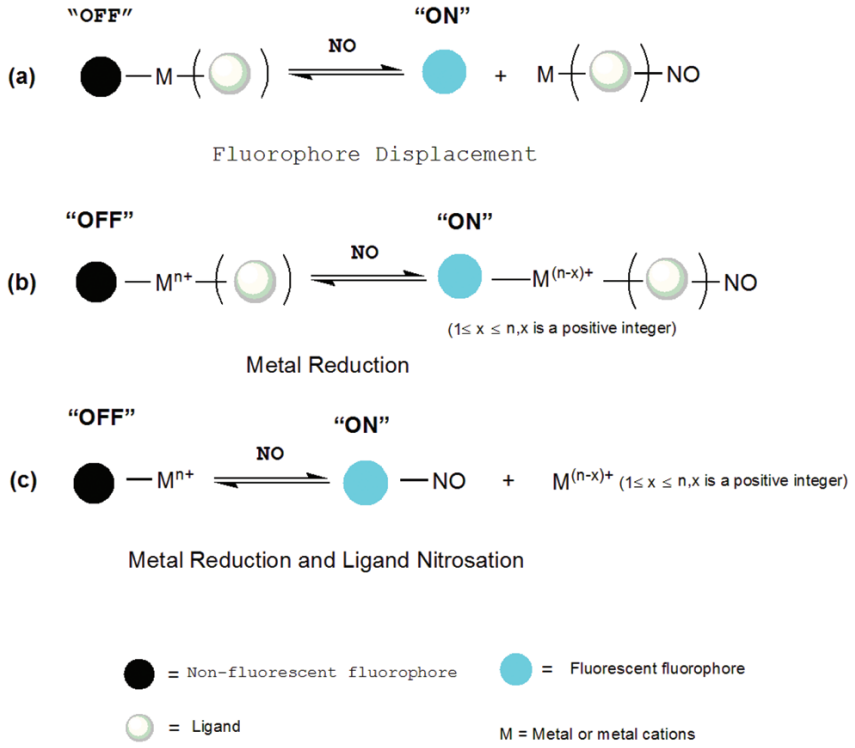

Figure 9. Strategies for generation of metal-transition probes. The fluorophore displacement (a), which accompanies NO binding to form a metal nitrosyl compound and release the ligand entirely or remove a chelating arm to a sufficient distance from the metal; the metal reduction (b) where the paramagnetic metal center is reduced to a diamagnetic pattern, restoring the fluorescence;(c) the most widely-used tactic of metal-tran- sition NO probes is implemented through both displacing the fluorophore and reducing the paramagnetic metal center by reductive nitrosylation of NO (Li and Wan, 2015).

Thus, fluorescent probes result easier to use associated with spatio-temporal NO concentration, moreover this probes have higher sensitivity to NO rather than its metabolites while the alternative methods described. Certainly the choice needs to be maid basing on the type of the study keeping attention to the quality of the samples will be analyze.

Aim of the study

Cancer immunotherapy mainly relies on the activation of the host immune system against tumors and it encompasses many approaches, such as tumor antigen–targeted monoclonal antibodies, immunological checkpoint inhibitors, cytokines, therapeutic cancer vaccines, and adoptive cell therapy (ACT). In particular, ACT consists in the transfusion of autologous tumor-specific T cells into tumor-bearing hosts, and to date, it represents a promising and realistic approach for the treatment of cancer patients. The effectiveness of ACT depends on several factors as the trafficking of adoptively transferred cells at the tumor site and importantly it requires overcoming the immunosuppressive tumor microenvironment.

Solid tumors so far accumulate immunosuppressive cells, such as myeloid derived suppressor cells (MDSCs) and tumor-associated macrophages (TAMs). MDSCs and TAMs are known to suppress T cell–mediated responses against cancer in several ways. One is based on the coordinated upregulation and activity of two specific enzymes: arginase (ARG1) and nitric oxide synthase type 2 (NOS2 or iNOS). At the tumor site, ARG1 induces the depletion of the amino acid L-arginine that is necessary for T cell activation and proliferation. NOS2 is responsible for the generation of nitric oxide (NO) and other reactive nitrogen species (RNS). These free radicals are known to impair T cell functions within the tumor. Nitric oxide has dual role in cancer biology because it can promote both tumor progression as well as tumor regression. NO induces tumor progression and metastasis by the direct induction of tumor-cell proliferation, migration and invasion, and indirectly through the expression of angiogenic and lymphangiogenic factors in tumor cells. On the other hand, high doses of NO have cytotoxic effects, which can result in tumor regression and metastasis inhibition. This dichotomous behavior mainly depends on the quantity, location, and timing of NO production and on the cellular sensitivity to this radical.

Therefore, the primary aim of this study was to investigate and characterize the impact of NOS2 on ACT, paying particular attention to NO, as its principal product. To this purpose, we performed *in vivo* experiments of ACT in either wild type or Nos2 knock-out mouse models, challenged with a tumor cell line expressing the OVA antigen.
Instrumental for dissecting the role of NO in ACT was the setting of a valuable tool to monitor in real-time NO release by confocal microscopy on viable tumor slices after T cell interaction. Specifically, we focused our attention to characterize the phenotype and functions of the specific cell population, responsible for NO induction following ACT in tumor-bearing hosts. Finally, to better characterize the molecular profile of this cell population, using a NO specific probe, we set-up a method to isolate this cell population from excised tumors by cell sorting.

Materials and Methods

Mice

C57BL/6 (WT), congenic CD45.1 (Ly5+) and OT-I transgenic mice were purchased from Charles River. The OT-1 mice in C57BL/6 background bear a transgenic T cell receptor, which allows the recognition of ovalbumin residues $OVA_{257-264}$ in the context of $H2K^b$. Pmel-1 transgenic mice in C57BL/6 background, which bear a Vα1Vβ13 H-2^b restricted TCR specific for murine melanoma peptide $gp100_{25-33}$ on $CD8^+$ T lymphocytes, were provided by Dr. N. Restifo (Surgery Branch, National Institutes of Health, Bethesda, MD).
Nos2$^{-/-}$ mice, *Cd40lg*$^{-/-}$ mice (B6.129S2-*Cd40lg*^{tm1Imx}/J) and *Tnfrsf5*$^{-/-}$ mice (B6.129P2-*Cd40*^{tm1Kik}/J) were all purchased from Jackson Laboratories. In this text for convenience *Nos2*$^{-/-}$ mice were named NOSKO, *Cd40lg*$^{-/-}$ mice were named CD40LKO and *Tnfrsf5*$^{-/-}$ mice were named CD40KO
Experiments were performed according to the national guidelines and approved by the local ethics committee.

Cell culture

EG7-OVA (H-2^b) cell line was derived from OVA-transfected EL4 thymoma cell line (Moore et al., 1988). Cell lines were grown in DMEM supplemented with 2 mM l-glutamine, 10 mM HEPES, 20 μM 2-mercaptoethanol, 150 U/ml streptomycin, 200 U/ml penicillin, G418 (0,4 mg/ml) and 10% heat-inactivated FBS (Invitrogen). Cells were maintained at *37*°C in a humidified atmosphere containing 5% CO2. Primary cells (myeloid cells sorted from tumors, $CD4^+$ or $CD8^+$) were cultured in DMEM supplemented with 2 mM l-glutamine, 10 mM HEPES, 20 μM 2-mercaptoethanol, 150 U/ml streptomycin, 200 U/ml penicillin and 10% heat-inactivated FBS (Biochrom). Lymphocyte culture was supplemented with recombinant IL-2 (20 IU/ml).
Synthetic peptides
Peptides: H-2 K^b-restricted OVA epitope (OVA257-264, SIINFEKL), the
H-$2D^b$-restricted $hgp100_{25-33}$ epitope (KVPRNQDWL), were all synthesized by JPT (JPT, Peptide Technologies, Germany). All lyophilized peptides were resuspended in DMSO (Sigma-Aldrich) and stored at –20°C until used.

Tumor challenge and Adoptive cells therapy (ACT)

C57BL/6 mice were s.c. injected on the right flank with $0{,}5x10^6$ EG-7-OVA cells. Tumor growth was monitored every 2 days by a digital caliper. 7 days later, when tumor area reached approximately 200 mm^3, mice were transferred i.v. with 0,5 $x10^6$ OVA-I specific CTLs, obtained from OT-I spleens. Briefly, spleens were harvested from OT-I mice and mechanically digested using the barrel from a 2 mL syringe, by pouring through a sterile metal cell-strainer. Splenocytes were seeded in 24-well plates in the presence of 1 μg/ml OVA-I peptide (Novartis, Basel, Switzerland) and maintained in culture for 7 days with 20 IU/ml IL-2.
6 hours after ACT, mice were injected i.p. with recombinant IL-2 (30,000 IU). IL-2 was administrated twice a day for three consecutive days. Mice were euthanized when tumors reached 1000 mm^3.

OVA-I specific CTLs were prepared from OT-I spleens. Splenocytes were plated in 24-well plates in presence of 1 μg/ml OVA-I peptide and 20 IU/ml IL-2 (Novartis, Basel, Switzerland). Cultures were maintained for 7 days in complete medium supplemented with 20 IU/ml IL-2. Data were presented as the percentage of survival after ACT.

Tumor dissociation

Mice were euthanized and tumors were surgically collected. Tumors were cut in small pieces with a scissor; pieces were covered with a digestive solution composed of collagenase IV (1 mg/ml) hyaluronidase (0,1 mg/ml) and DNase (0,03 KU/ml) and incubated at 37°C; every 10 minutes tumors were mechanically processed using a 5 ml pipette. After 1 hour, cells were collected and washed in complete medium twice to remove all digestive solution.

Cytofluorimetric staining and analysis

Cells isolated from tumors and spleens were washed in PBS and incubated with anti-Fc-γ receptor for 10 minutes at 4 °C to reduce unspecific binding. Samples were then stained with antibodies or relative isotype controls for 20 minutes at 4°C, washed in PBS and finally resuspended in 300 μl of PBS for flow citometry. The antibodies used were: anti-CD11b PE-Cy7 (clone M1/70, BD catalogue no. 552850), anti-LY6G APC-Cy7 (clone 1A8, BD catalogue no. 560600), anti-CD11c APC (clone HL3, BD catalogue no. 550261), anti-I-A/I-E PerCP-Cy5.5 (clone M5/114.15.2, BD catalogue no. 562363), anti-TNFα FITC (clone MP6-XT22, BD catalogue no. 554418), anti-CD45.1PE (clone A20, BD catalogue no. 12-0453-83), anti-CD8 PerCP-Cy5.5 (clone 53-6.7, BD catalogue no. 45-0081-82), anti-LY6C eFluor 450 (clone HK1.4, BD catalogue no. 48-5932-82), anti-F4/80 FITC (AbDSerotec, clone CI:A3-1, catalogue no. MCA497FB), FAB5538PRabbit anti-mouse NOS2 (Abcam, polyclonal catalogue no.15323). To analyze the intracellular staining of NOS2, anti-rabbit Rhodamine Red X antibody (Jackson Immune Research, catalogue no. 711-295-152) was used. BD Citofix/Cytoperm Kit was used for intracellular staining. TNF and INF-γ were detected using anti-TNFα FITC (clone MP6-XT22, catalogue no. 554418) and anti-INF-γ FITC (clone XMG1.2, catalogue no. 554418) both from BD. Aqua Live/Dead®dye (Invitrogen) was used to analyze cell viability. Flow data were acquired with a LSRII FACS (BD Biosciences) and analyzed with FlowJo (Tree Star, Inc.) software.

Cell sorting

Total cell suspension from tumors were stained with: anti-CD11b PE-Cy7, anti-LY6G APC-Cy7, anti-I-A/I-E PerCP-Cy5.5, anti-LY6C eFluor 450, anti-F4/80 FITC for 20 minutes; cells were washed and resuspended in FACS buffer (PBS, EDTA 0.5 mM, FBS 3%, 150 U/ml streptomycin, 200 U/ml penicillin) and sorted using FACS Aria® (BD Biosciences).

NO detection within viable tumor slices

C57BL/6, NOS2 KO, CD40L KO and CD40KO mice were s.c. injected with 0.5 × 10^6 EG7-OVA cells. At day 7, tumors were dissected, embedded in 6% agarose and cut on vibratome (Leica, VT1000S) to obtain thick viable tumor slices (250

μm). Slices were loaded with the NO fluorescent probe (diaminorhodamine-4M AM; Sigma) for 1 hour at 37°C. CFSE-labeled $CD8^+$ T cells (1.2×10^6) were added on the top of tumor slices. After 2 hours, tumor slices were fixed with 4% PFA for 30 minutes at RT. Nuclei were counterstained with 1 μg/ml ToPRO. Slides were mounted with ProLong (Invitrogen) and analyzed by confocal microscopy (TCS SP5, Leica).
For quantitative analysis of NO staining, different and noncontiguous regions of interest (50 ROIs) were randomly selected, and DAR-4M AM mean intensity was quantified for each ROI. Results were expressed as fold induction over control (no $CD8^+$ T cells). Recorded images were processed with Vimmaging developed under MATLAB™ (MathWorks, Natick, MA), and WCIFImageJ v1.35.

CFSE cell labeling

OT-I/CD45.1 splenocytes, EG7 cells (for proliferation assays) and $CD8^+$ T lymphocytes, derived from the spleen of either OT-I or Pmel-1 mice (for NO detection), were labeled with carboxyfluorescein succinimidyl ester (CFSE, CFSE- Cell Trace Kit, Invitrogen Molecular Probe) according to manufacturer's instructions.

Immunomagnetic sorting

$CD11b^+$ cells were isolated for positive selection from spleens and tumors with anti-CD11b MicroBeads (MiltenyiBiotec, Germany). $Ly6G^-$ $CD11b^+$ cells were isolated from tumors by first depleting Ly6G-positive cells by using the anti-Ly6G MicroBead Kit (MiltenyiBiotec). The negative fraction, Ly6G-$CD11b^+$ cells, was indeed decanted and in some experiments Ly6G-$CD11b^+$ cells were co-cultured with 0.1×10^6 CFSE-labeled EG7 cells at 3:1; 2:1; 1:1 ratios for 24 h. Spleens and lymph nodes from tumor-free or EG7 tumor-bearing mice were used to separate $CD8^+$ T lymphocytes by using CD8α+ T cell isolation negative Kit (MiltenyiBiotec). $CD4^+$ naïve T lymphocytes were isolated from spleens of OT-II mice using a $CD4^+$ T cell isolation Kit (MiltenyiBiotec). All separations were performed according to manufacturer's instructions by using Midi Macs columns (MiltenyiBiotec). Purity of cell populations was evaluated by flow cytometry and exceeded 90%.

Antigen presentation assays

Myeloid cells ($CD11b^+Ly6G^-$) from EG7-bearing mice - either treated or not with ACT- were co-cultured with 5×10^4 naïve $CD4^+$ T lymphocytes isolated from OT-II mice by immunomagnetic cell-sorting as previously described in a U-bottom-96 well plate for 72h. Supernatants from co-cultures were collected and assessed for the concentration of mouse IFN-γ.

ELISA

Supernatants from co-colture experiments (myeloid cell subpopulations sorted from tumors, treated or not with ACT plus T lymphocytes) were collected after 72h. Than IFN-γ production was measured using mouse IFN-γ ELISA Kit sandwich (DY485 R&D Systems, Minneapolis, MN). The assay was performed according to manufacturer's instructions.

NO detection on tumor cells by flow cytometry and cell sorting

Tumors were disaggregated as described above by enzymatic digestion. In this case, the enzymatic mixture was supplemented with 5 µM of the NO fluorescent probe DAF- FM Diacetate (4-Amino-5-Methylamino2',7' Difluorofluorescein Diacetate) (Invitrogen). Tumor single cell suspension was subsequently washed in PBS, resuspended in PBS supplemented with 1% heat-inactivated FBS (Invitrogen). Incubated with anti-Fc-γ receptor for 10 minutes at 4 °C to reduce unspecific binding. Cells were labeled for 20 min at 4°C with the following antibodies: anti-CD11b PE-Cy7, anti-Ly6C eFluor 450, anti-Ly6G APC-Cy7 and finally sorted using FACS ARIA cell-sorter, using the gating strategy showed below.

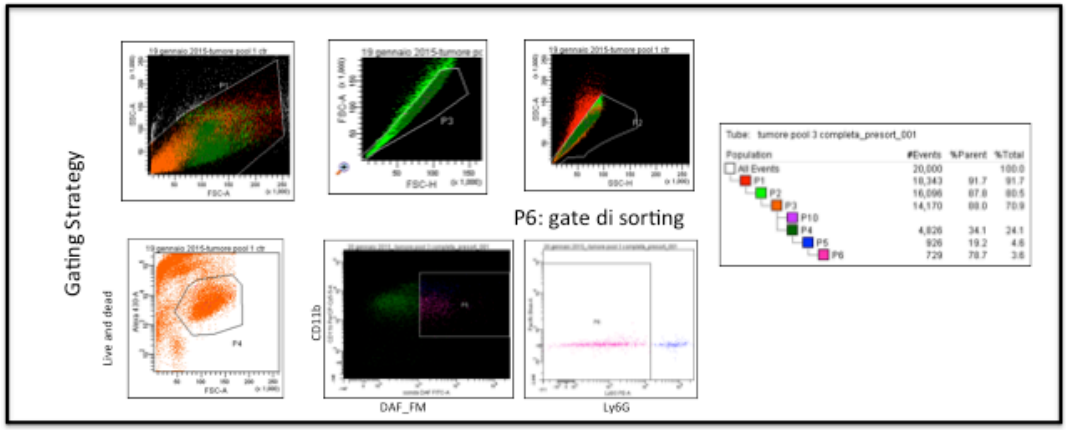

The population of interest was CD11b^{+}DAF-FM^{+} Ly6G^{-} within live cells. For dead cell exclusion, samples were stained with Aqua Live/Dead®dye (Invitrogen).

Gene expression

Total RNA was isolated from CD11b^{+}DAF-FM^{+} Ly6G^{-} cells, isolated from tumors at day 3 after ACT using TRIzol reagent (Life Technologies, CA, USA). RNA integrity assessed using Agilent-2100-Bioanalyzer (Agilent Technologies, CA, USA). cDNA from samples was amplified and total RNA was purified with Ovation Pico WTA System V2 (NuGEN, CA, USA). Samples were hybridized to Affymetrix Mouse Genome 430 2.0 arrays and scanned with an Affymetrix GCS 3000 7G scanner.

Myeloid cell data collection and processing

Myeloid NO producing cells CD11b^{+}DAF-FM^{+} Ly6G isolated from tumors at day3 after ACT were collected and merged with 3 publicly available datasets comprising microarray data of tissue macrophages (twelve samples), tissue dendritic cells (twelve samples), and monocytic myeloid-derived suppressor cells (nine samples). All data were measured on Affymetrix arrays and have been downloaded from Gene Expression Omnibus (http://www.ncbi.nlm.nih.gov/geo) or obtained by the authors of the original publications.

The complete list of datasets is provided in Table 1. Microarray probe fluorescence signals of samples belonging to the same platform were converted to expression values using robust multiarray average procedure RMA (Irizarry et al., 2003) of Bioconductor affy package. Specifically, fluorescence intensities were background-adjusted and normalized using quantile normalization. log2 expression values were calculated using median polish summarization and custom chip definition files for a total of 21115 custom probe sets for Mouse Gene 1.0 ST Array based on Entrez genes (mogene10st_Mm_ENTREZG version 19.0.0) (Dai et al., 2005) and 17856 custom probe sets for Mouse Genome 430 2.0 Array based on Entrez genes (Mouse4302_Mm_ENTREZG version 19.0.0). All data analyses were performed in R version 3.1.3 using Bioconductor libraries and R statistical packages. Microarray data of Tip-DCs are available in GEO and the accession number is GSE74427. Data of the myeloid cell collection hybridized on Mouse Gene 1.0 ST Array were concatenated with those hybridized on Mouse Genome 430 2.0 Array, matching 16 742 Entrez gene IDs, i.e. the common identifier of custom probe sets in both data sets. A direct merging of raw CEL files, although desirable for an efficient removal of batch effects, was unfeasible due to the different probe sequences of Mouse Gene 1.0 ST and Mouse Genome 430 2.0 arrays. The combined matrix was subjected to ComBat (Johnson et al., 2007) to remove batch effect. ComBat was applied with default parameters with the exception of the adjustment variables that were imputed as a vector of platform type labels.

GEO series	Platform	GEO samples	Reference
GSE15907	Mouse Gene 1.0 ST	GSM605850, GSM605851, GSM605852, GSM605856, GSM605857, GSM605858, GSM605862, GSM605863, GSM605864, GSM538239, GSM538240, GSM538241, GSM605823, GSM605824, GSM605825, GSM854273, GSM854274, GSM854275	a
	Mouse Gene 1.0 ST	EA07068_226626, EA07068_226627, EA07068_226628, EA07068_226638, EA07068_226639, EA07068_226640, EA07068_226649, EA07068_226650, EA07068_226651	a
GSE42061	Mouse Genome 430 2.0	GSM1031725, GSM1031726, GSM1031727	b
GSE17322	Mouse Genome 430 2.0	GSM433363, GSM433365, GSM433367	c
In-house	Mouse Genome 430 2.0	Tip_DC_A, Tip_DC_B	--

Table 1. Complete list of gene expression datasets used in this study and their sources.
a. Immunological Genome Project (www.immgen.org). b. Lei L, Li H, Yan F, Xiao Y. Hyperlipidemia impaired innate immune response to periodontal pathogen porphyromonas gingivalis in apolipoprotein E knockout mice.PLoS One 2013;8(8):e71849. c. Edelson BT, KC W, Juang R, Kohyama M et al. Peripheral CD103+ dendritic cells form a unified subset developmentally related to CD8alpha+ conventional dendritic cells. J Exp Med 2010 Apr 12;207(4):823- 36.

Cluster and differential gene expression analysis

Sample grouping was obtained using hierarchical clustering with Pearson correlation and centroid as distance metric and linkage, respectively. The expression matrix of the myeloid cell collection were analysed with the Significance Analysis of Microarray method (SAM)(Tusher et al., 2001), coded in the samrRpackage (http://cran.r- project.org/web/packages/samr/index.html) to identify differentially expressed genes in the comparisons between subsets of macrophages, dendritic cells, and monocytic myeloid-derived suppressor cells (33 samples). These genes were identified using the multiclass procedure of sam Bioconductor package. The q-value threshold was set to 0, the contrast among the

three classes was imposed to be different, and the SAM multiclass score was set ≥ 2. The multiclass analysis resulted in a list of 604 differentially expressed genes (Table2) among macrophages, dendritic cells, and monocytic myeloid-derived suppressor cells.

Gene signature comparisons

Gene expression profiles of the tissue DCs, tissue MFs, M-MDSC and Tip-DCs were compared using the published genes signatures of DCs (Miller et al., 2012), MFs (Gautier et al., 2012) and M-MDSCs (Conde et al., 2015).

	Gene Symbol
Genes up regulated in tissue MFs	Acp1, Adh5, Adss, Ampd3, Anxa3, Anxa4, App, Ate1, Atp1b3, Atp6v1a, Glb1, Bmi1, Calu, Capg, Casp1, Cd151, Scarb2, Cd37, Comt, Ctsd, Ctsl, Ctss, Dpm1, Ecm1, Emr1, Chchd2, Evi5, Ptk2, Aktip, Grk5, Grcc10, Grn, Hpse, Impact, Itgb1, Itm2b, Kif16b, Anxa1, Lrp1, Mgat1, Ninj1, P2rx4, Ppp3ca, Pros1, Pts, Rab12, Rab18, Rabggtb, Rad17, Rbpms, Rxra, Sorbs3, Vps4b, Smpd1, Soat1, Syngr1, Ube3a, Map2k5, Clcn7, Rcn2, Add3, Naglu, Spg21, Rnf11, Timm10, Pdlim4, Fbxw7, Nus1, Camk1, Ifi27, Vamp4, Rragc, Golga4, Akr1e1, Nagk, Apip, Serinc1, Socs5, Vapb, Sec11a, Pf4, Bcam, Ccdc126, Krcc1, Ndfip1, Zak, Ogfod3, Ahnak, Pgpep1, Tceanc2, Aggf1, Hiatl1, Uba5, Acot13, Dnajc10, Mfsd1, 2610002M06Rik, Ift27, Ptgr1, Dynlt3, Herc4, Abhd5, Saysd1, Mrpl18, Mrpl24, Pcnxl4, Fam114a2, Caap1, Yipf4, 1600012H06Rik, Col4a3bp, Tsr3, Steap3, Tmem140, Lamtor5, Ak8, Mcts1, Snx4, Snx24, Afg3l2, Trim32, Mettl7a1, 2010107E04Rik, Fra10ac1, March8, Cdadc1, Paqr7, Fbxl20, Slc16a10, Tmem87b, Tmem55a, Adipor1, Zfp839, Fblim1, Gorasp1, Zfp943, Arhgap12, Nln, Zdhhc20, Snrnp35, Abca6, Glt8d1, Mtif2, Spopl, Arsk, Kidins220, Stxbp5, Fam20c, Sacm1l, Fam126a, Emc9, Gopc, Rabif, Clp1, Rusc2, Slc44a1, Zfp120, Slc16a6, Jkamp, Cdk20, Ano6, Mat2b, Slc35b3, Cds2, Elac1, Bloc1s4, Acap3, Slc25a36, Kbtbd2, D15Ertd621e, Pank3, Tmem18, Cd300a, Cd300ld, Gm527, Zfp758, Tbc1d24, Fez2, Pggt1b, Rab3gap1, BC003331, Ndufs1, Dolk, Sestd1, Slc25a24, Ppp4r2, Pyroxd1, Zfp790, Tmem159, BC030336, Zfp958, Slc36a4, Tmem205, Zbtb6, Dagla, Mbtps2, Flnb, Nt5dc1, Plekhm1, Slc38a6, Wfdc17
Genes up regulated in tissue DCs	Adam19, Asgr2, Cd34, Mark2, Fyn, H2-Oa, H2-Ob, Hivep2, Il10ra, Il18rap, Napsa, Klrd1, Lrrfip1, Ltb, Pak1, Rel, Ccl22, Ccl4, Skil, Slc2a3, Spn, Zyx, Gadd45g, Icosl, Tbc1d8, Gps2, Fam129a, Fam107b, Abhd15, Slc38a2, Dusp16, Tbc1d9, Taf4b, Ddit4, Sesn3, Rnase6, Sf3b1, Kmo, Slamf9, Plekhg2, Spty2d1, Haao, Plekha5, Lmo1, Elmo1, Bmp2k, Dock10, Mgl2, Slc25a25, Ppp1r16b, Tspan33, Elmsan1, Malt1, Itga8, Nfkbid, Arhgef40, Gpr4, Adrbk2, Fbrsl1, Itprip, Fam71a, Ctnna1, Chd1, Clk1, Dhx15, Ddx3x, Eif3a, Eps15, Gas5, Hfe, Ikbkb, Mcl1, Ints6, Rock1, Sub1, Uimc1, Stag1, Slk, Top2b, Zfp62, Ubl3, Ddx3y, Azin1, Ccnl2, Srsf4, Hnrnph1, Tspan13, Sltm, Rbm25, Paxbp1, Dhx40, Chd1l, Rraga, Gtpbp4, Spag9, Nipbl, Tbc1d5, Pan3, Actr3, Rnd3, Cyld, Hnrnpm, Wsb1, Phip, Cd163, Ddx50, Zc3h7a, Rsrc2, Zcchc6, Ubxn7, Safb2, Rsf1, St8sia6, Chd2, Tacc1
Genes up regulated in M-MDCs	Aif1, Aldoc, Arg2, Bub1, Ccnb2, Ccne1, Ccne2, Ccnk, Cdk1, Cdh1, Ch25h, Plk3, Cst7, Atn1, Eif4ebp2, Foxm1, Cdca3, Gtpbp1, Htr7, Itga5, Jak3, Lyn, Mcm2, Mcm5, Nab2, Ndrg1, Nfatc3, Orc1, Osm, Pafah1b3, Pfn1, Plau, Plk1, Pole, Psme3, Ptbp1, Kif20a, Rrm2, Sf3a2, Scd2, Ccl12, Ccl2, Ccl7, Sh3bp1, Slc2a1, Aurkb, Suv39h1, Tbrg4, Trp53, Tyms, Usp10, Med14, Pald1, Smtn, Gtse1, Ccdc97, Cdca8, Cks1b, Spag5, Phc2, Extl3, Cxcl11, Ube2j1, Aldh18a1, Fads2, Gosr2, Clec4n, Brd4, Trem1, Trem3, Foxj2, Gpr35, Cenpm, Nacc1, Fip1l1, Asf1b, Pmf1, Gatm, Mastl, Eri1, Dcakd, Ifitm1, Nabp2, Mcm10, Kif18b, Crtc3, Nup205, Cenpn, Mvb12b, P2ry13, Pgs1, 8430419L09Rik, Ocstamp, Fam46c, Dhcr24, Taf1d, Dcp1a, Fads1, Ppp1r18, Dtl, Ticrr, Btbd19, Troap, Olfml3, Ifi44, Noc4l, Eogt, Pom121, Shmt2, Nusap1, E2f8, Slc13a3, Fanci, Proser1, Ncaph, Ube2d1, Git1, Gatad2b, Eva1b, Gdpd5, Spon1, 2900026A02Rik, Eme1, Lsm12, Aak1, Zfp384, Mthfd1l, Prr11, Gins2, Treml2, Nol4l, Htra4, Nckap5l, Gpr114, Opa3, Gnptab, Aprt, Atpif1, Phb2, Bsg, Cdk4, Cox8a, Slc25a1, Ercc3, Gamt, Bloc1s1, Bscl2, Hdac3, Hus1, Ndufs4, Ndufv1, Mrpl40, Pde6d, Prep, Rab5c, Polr2j, Rsu1, Slc7a7, Spp1, Tfec, Mlx, Tpi1, Tsta3, Vdac1, Psmc4, Psmb2, Mrpl15, Nagpa, Imp4, Yipf3, Vps25, Pde7b, Commd2, Sgta, Dnlz, Mtx2, Clpp, Rcan3, Nme6, Eif3i, Ift20, Mrpl19, Arl2, Gabarap, Cript, 0610007P14Rik, Repin1, Trappc2l, Mrps24, Nif3l1, Dap3, Atp5d, Krtcap2, 1110008L16Rik, Grina, Chchd5, Ndufb9, Cox16, Smim8, Isoc1, Ccdc90b, 2310022A10Rik, Nmnat1, Rnf181, Tpgs2, Spryd4, Adat2, Mrpl33, Kdelr2, Tbc1d7, Cuedc2, Ndufa10, Ccdc53, Snrpd3, Sdhb, Ost4, 1700021F05Rik, Akr1b10, Slc25a11, Rps27l, Fam96a, G6pc3, Phf5a, Mphosph6, Cebpzos, Samm50, Tmem214, Gmppa, Manbal, Commd10, Psmg4, Med6, Tmem147, Polr2f, Dhdh, Trnau1ap, Mad2l2, Jmjd8, Zbed3, Pgm2, Ppme1, Ndufv2, Cenpv, Thoc3, Isca2, Slc35f6, Ndufs7, Malsu1, Grhpr, Yif1b, Desi2, Ifitm2, Kremen1, Mrpl34, Kti12, Zfand2a, Brk1, Rars, Adi1, Dph3, Nsun3, Cyb5r3, Cox6b1, Fam57a, Pip4k2c, Parvb, Cep78, Tfe3, Mtmr9, Fam20b, Dhrs7b, E430025E21Rik, Alg12, Mettl8, Psmf1, Msto1, Prune, Efcab14, Dera, Alkbh6, Mettl22, Fcgr4, Ccdc32, Gdpgp1, Ttll1, BC031181, Heatr2, Gm5617

Table 2. Complete list of the genes differentially expressed between tissue dendritic cells, tissue macrophages and M-MDSCs.

Generation of polyclonal CD40L KO CD8$^+$ T cells recognizing OVA

WT and CD40LKO mice were intraperitoneally injected with 100 μg of FGK45.5 antibody against CD40 (BioXcell, NH 03784-1671 USA), in association with with $OVA_{257-264}$ (SIINFEKL) peptide (200 μg/mouse) administration at the tail base and then rubbed with imiquimod (Meda, Sweden). Peptide injections were repeated twice every 7 days.

Statistic analysis

Values are reported as mean ± standard error (SE). Survival experiments are reported as Kaplan-Meyer curves and significance was determined with log-rank test. Student's t-test was performed on parametric groups. Values were considered significantly with $p \leq 0,05$ and are indicated as *=$p \leq 0,05$; **=$p \leq 0,01$ and ***=$p \leq 0,001$.4

Results

The impact of NOS2 on adoptive cell therapy

ACT represents a promising approach to treat cancer patients. ACT consists in the transfer of $CD8^+$ T lymphocytes specific for tumor antigens. The effectiveness of this therapeutic approach requires overcoming of the immunosuppressive tumor microenviroment, where distinct immune cell subsets as TAMs and MDSCs, definitely block T cell functions (Ugel et al., 2015).

A key inhibitory pathway in the tumor microenvironment involves the metabolism of ariginine through regulated expression of ARG1 and NOS2(Gabrilovich et al., 2012). Nonetheless, the precise role of ARG1, NOS2 and their bioproducts in cancer remains controversial. In particular, the contribute of NOS2 in either promoting or controlling tumor progression is likely dependent on the cell types up-regulating the expression of this enzyme and the relative NO concentration within the tumor microenvironment.

Indeed, we moved to investigate the role of NOS2 and NO in cancer immunotherapy.

Specifically, to understand the role of NOS2 on ACT, we performed *in vivo* experiments in either WT or NOSKO mice models. Indeed, we challenged mice with a cell line expressing the ovalbumin (OVA) antigen EG-7-OVA; at day 7, when tumor volume reached 100 mm^2, we adoptively transferred *in vitro* activated, congenically-marked, OVA-specific $CD8^+$ T cells and we monitored animal survival followed by ACT (Figure 1A). We observed a substantial impairment of ACT in NOSKO mice; our data showed, indeed, half survival of NOSKO mice after lymphocyte infusion (Figure 1B). This result was unexpected, especially for the well-known suppressive role of NOS2, which blocks T cell proliferation and activity in the tumor microenviroment.

To clarify these data, we checked by cytofluorimetric analysis the recruitment of OVA-specific $CD8^+$ T cells at the tumor site and spleen of tumor-bearing mice undergoing ACT. Higher percentages of OVA-specific, $CD8^+$ $CD45.1^+$ T cells were recovered in NOSKO compared to WT mice, both in the spleen and tumor (Figure 1C). Transferred $CD8^+$ T cells also produced higher amounts of IFNγ in NOSKO mice compared to wild type mice in the tumor microenvironment, while we observed less activity of CD8+ T cell in the spleens from either WT and NOSKO bearing-mice compared with healthy WT (Figure 1D).

Nonetheless, although the NOS2 deletion significantly enhanced T cell recruitment and activity within the tumor, this was not sufficient to improve the efficacy of ACT. These data suggest that NOS2 expression represented a non-redundant and essential element to achieve the therapeutic effect of ACT in tumor-bearing hosts. Taken together these observations indicated that NOS2 is necessary for tumor rejection and suggest a remodelling of tumor microenviroment after ACT.

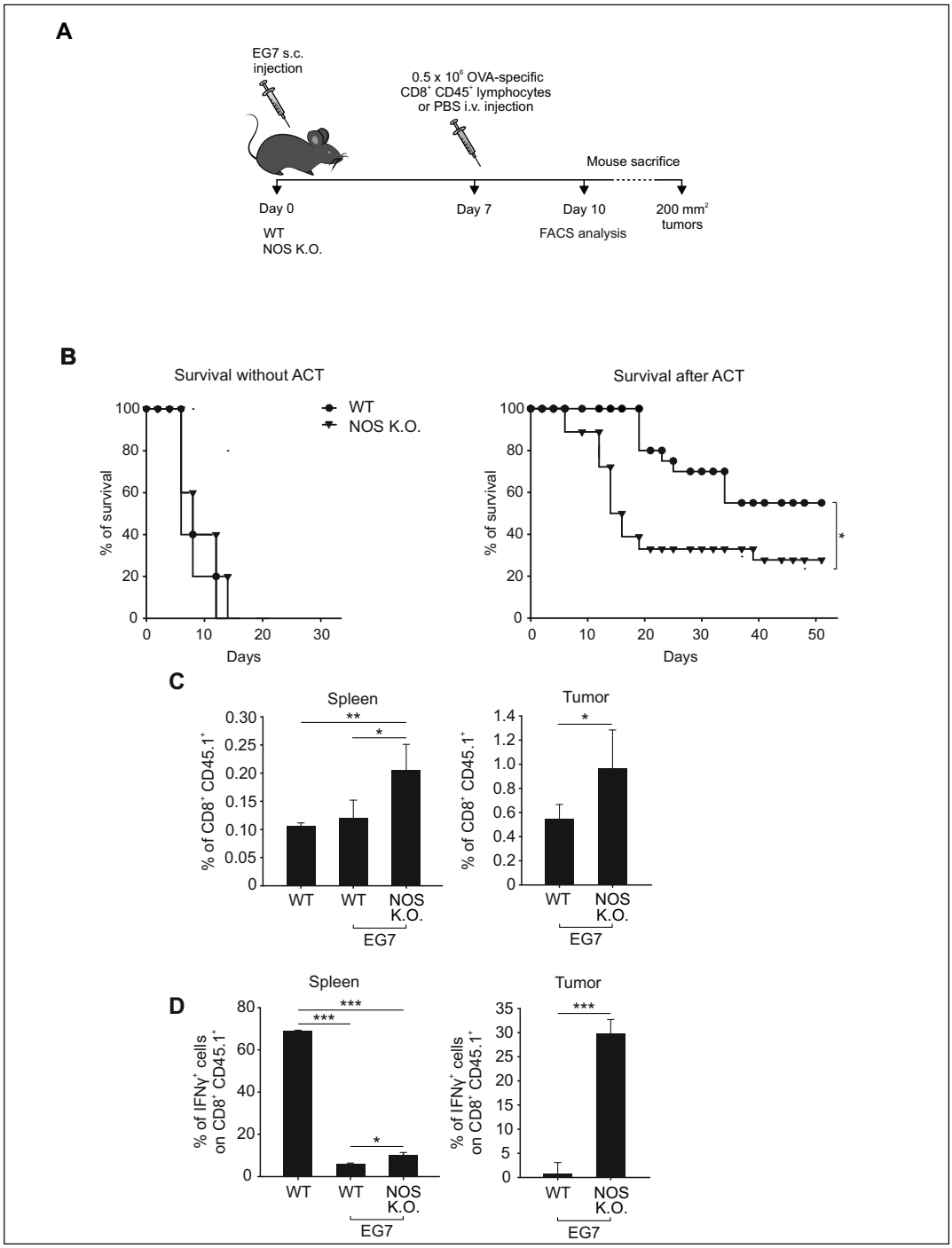

Figure 1. The impact of NOS2 on ACT

(A) Timeline for experimental treatment. WT and NOSKO mice were injected with EG7-OVA cells. At day 7, mice were either treated or not with OVA-specific, $CD8^+CD45.1^+$ lymphocytes obtained from OT-I mice. Mice were euthanized i) at day 10 (to perform FACS analysis and cell sorting) or, ii) when the tumor reached an area of 200 mm^2, for survival experiments. (B) WT and NOSKO EG7-OVA tumor-bearing mice were left untreated (n=5) or treated with ACT with OVA-specific CTLs (WT n=20; NOS KO n=18). Long- rank test statistic * $P<0.05$. (C) Percentage of OVA-specific $CD8^+CD45.1^+$ lymphocytes in spleens (left) and tumors (right) either from WT or NOS KO mice, challenged with EG7-OVA and undergoing ACT. (D) Percentage of $^+CD8^+$ $CD45.1^+IFN\text{-}\gamma^+$ cells from spleens (left) and tumors (right) from either WT or NOSKO mice undergoing ACT (N=4), stimulated ex vivo with the OVA peptide. Error bars are mean ± s.d. ***$P\leq0.001$, **$P\leq0.01$ and *$P\leq0.05$, unpaired Student t-test.

NO production within the tumor microenviroment

Given the rationale from our *in vivo* experiments, we hypothesized a possible role for NO, as it represents the principal product of NOS2 activity. At the tumor site, NO can either facilitate or inhibit tumor progression and metastasis by direct induction of tumor-cell proliferation, migration and invasion, and indirectly through the expression of angiogenic and lymphangiogenic factors in tumor cells. On the other hand, high doses of NO have cytotoxic effects, which can result in tumor regression and metastasis inhibition. This dichotomous behavior mainly depends on the quantity, location, and timing of NO production and on the cellular sensitivity to this radical (Fukumura et al., 2006).

Indeed, to better understand which function NO can exert in ACT, we analyzed NO dynamics within the tumor microenvironment in the presence or absence of tumor-specific T lymphocytes. To this aim, we set up a technique for NO detection in viable tumor slices taking the advantage of the specific fluorescent probe DAR-4MAM.

DAR-4M AM is an organic-based fluorescent NO probes, mostly composed of two elements: a NO-reactive moiety and a fluorophore. The NO-reactive moiety (an ammine and a methylamine) act as a modulator in the photoinduced electron transfer (PeT) mechanism, which quenches the fluorescence of fluorophores (rhodamine) until it binds with the NO or NO oxidized products. The ammine and methylamine groups are rapidly hidrolyzed by cells' esterases and after the bound with NO the rhodamine became fluorescent. DAR 4M AM florescence is stable under intraceullar ph and it can detect little concentration of NO as 7nM (Li and Wan, 2015).

Our protocol is based on the inclusion in agarose of fresh tumors expressing the specific antigen OVA. Subsequently, we cut the embedded tumor with the vibratome to obtain viable slices of 250μm. Tumor-slices were loaded with DAR-4M-AM at 5uM and incubate in the presence or absence of $CD8^+$ T lymphocytes, either specific or not for the OVA tumor antigen (Figure 2A). Tumor-slices loaded or not with T lymphocytes, were incubated for 2 hours at 37°C; at the end of the incubation, tumor-slices were fixed mounted and analysed by confocal microscopy. For quantitative analysis of NO staining, different and noncontiguous regions of interest (50 ROIs) were randomly selected, and DAR-4M AM mean intensity was quantified for each ROI. Results were expressed as fold induction over control (no $CD8^+$ T cells).

We applied this method to measure NO production and release in viable tumor slices, obtained from either wild type or NOSKO tumor-bearing EG-7-OVA mice (Figure 2B).

Interestingly, we observed that a significant induction of NO release occurred as the result of the addition of antigen-specific $CD8^+$ T cells on viable tumor slices. On the contrary, the addition of antigen-unrelated T cells to tumor slices did not trigger the NO burst. Coherently, our data also confirmed that NOSKO tumor slices presented a significant reduction in NO release compared to the wild type, even in the presence of activated antigen-specific lymphocytes (Figure 2C).

Thus our in vitro data suggested that the interaction between activated anti-tumor CD8+ T cells within the tumor microenviroment triggered NO release which is primarily produced by the NOS2 enzyme, highly express by myeloid cells.

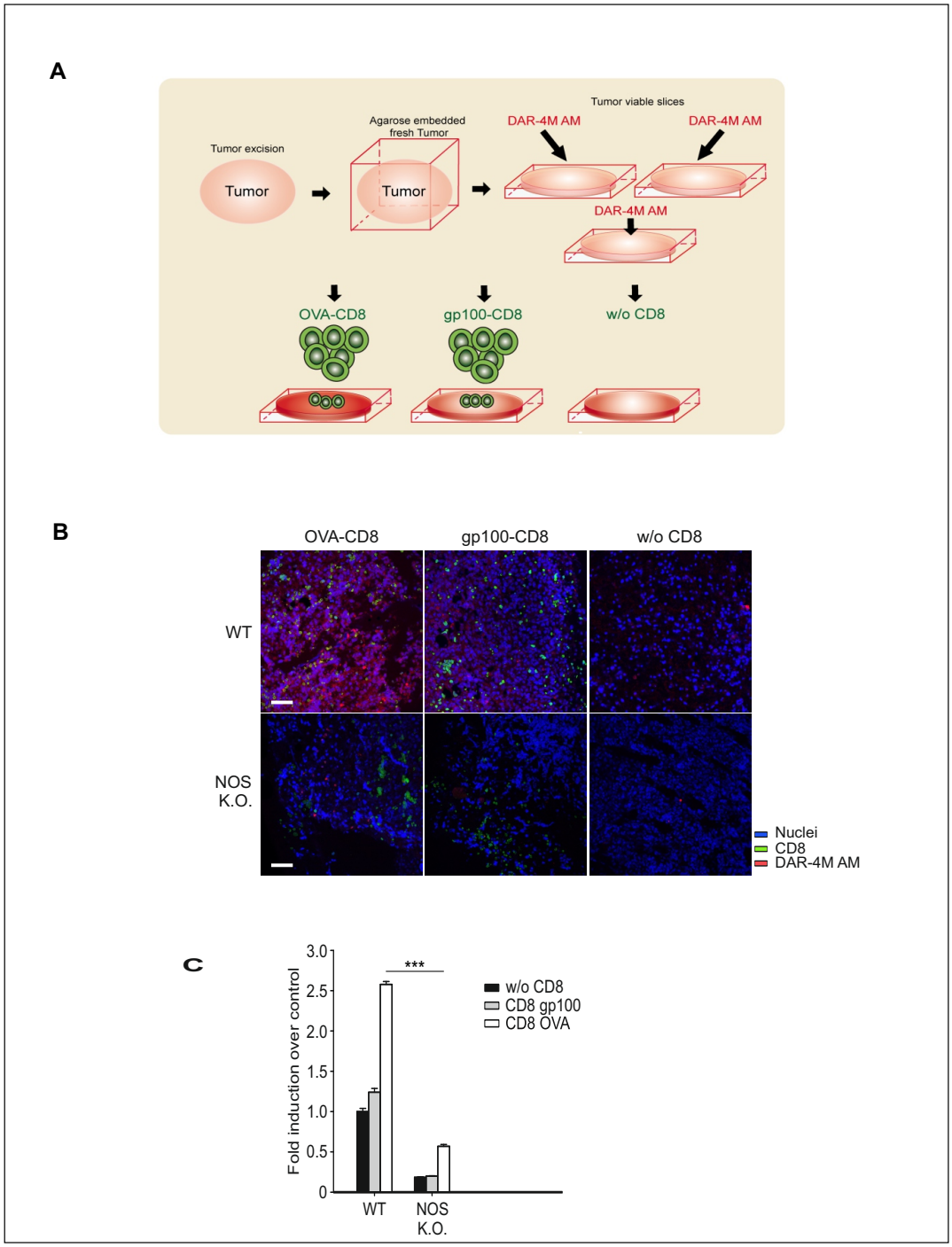

Figure 2. NO detection within tumor slices

(A) At day 7 post implant, EG7 tumors were dissected, embedded in agarose and cut with a vibratome to obtain viable tumor slices (250 µm). Slices were loaded with DAR-4M AM probe, which detects NO. CFSE-labeled T cells specific for either OVA or gp100 antigen were added on the top of tumor slices. After incubation, tumor slices were fixed and analysed by confocal microscopy.

(B) Representative images of NO production after T cell interaction within viable tumor slices. From the left: NO production (red) in the presence of OVA-specific $CD8^+$ T cells (green, OVA-CD8), gp100-specific $CD8^+$ T cells (green, gp100-CD8) or in the absence of $CD8^+$ T cells (w/o CD8). Top: tumor slices from WT mice; bottom: tumor slices from NOS K.O. mice. DAPI (blue). Scale bar, 50 µm.

(C) Released NO levels were measured as mean of fluorescence expressed as fold induction over the control (w/o CD8). Error bars, mean ± s.e.m. ; (n=12, pooled from 3 independent experiments), *** $p \leq 0.001$, unpaired Student t-test analysis.

NOS2 and NO shape tumor microenviroment following ACT

In tumor-bearing hosts, NOS2 enzyme activity is mostly upregulate in myeloid cells as TAMs and MDSCs, capable to suppress T cell activity. Indeed, we decided to analyze the myeloid compartment in the tumor microenvironment before and after ACT. We first investigated changes in the number and phenotype of intra-tumoral myeloid cells. We started looking at the entire myeloid cell subset, infiltrating tumors on the day 10-12 post tumor implant and we observed no changes on the percentage of tumor-infiltrating $CD11b^+$cells in either WT or NOSKO mice (Figure 3A). We thus evaluated changes within the myeloid cell fraction. For this pourpouse, we first expanded the phenotypic characterization of this cell population by flow cytometry either in wild type or NOSKO mice before and after immunotherapy (Figure 3B). Interestingly, we observed an expansion of $CD11b^+NOS2^+$ cells in wild type tumors, which was absent in NOSKO mice after ACT. Moreover, among the $CD11b^+$ $Nos2^+$ cell fraction, we observed an increased number of $Ly6C^+MHCII^+$ cells with a coincident reduction in $F4/80^+$ macrophages (Figure 3B-C), suggesting that NOS2 activity was primarily due to the $Ly6C^+MHCII^+$ cell fraction. Afterward, we analyzed the functional activity of this myeloid cell subset. We focused our attention on WT mouse model, where we found the expansion of $CD11b^+NOS2^+$ cells after ACT. Indeed, we challenged mice with the EG-7-OVA cell line and we sorted $CD11b^+Ly6C^+MHCII^+$ or $CD11b^+F4/80^+$ cells from tumors, treated or not with ACT, to perform functional assays.

We first stimulate the two populations with lipopolysaccharide (LPS) to evaluate their ability to release TNFα in response to exogenous stimuli (Figure 4A).

We found that only the $CD11b^+NOS2^+Ly6C^+MHCII^{++}$ cells were able to secrete TNFα after LPS stimulation; we also observed that this capability was higher on cells derived from tumors treated with ACT. Since TNFα is a hallmark of activated myeloid cells, we took into consideration the cytostatic activity of this cell population against tumor cells. Indeed, we performed co-colture experiments by culturing $Ly6G^-CD11b^+$ cells - isolated from tumors of mice adoptively transferred with tumor-specific $CD8^+$ T lymphocytes- with tumor cells (Figure 4B). We found that $Ly6G^-CD11b^+$ isolated from wild type mice treated with ACT showed enhanced cytostatic activity compared to NOSKO mice. The tumoricidal action of this myeloid cell subset was accompanied by an increased NOS2 expression in cells $CD11b^+Ly6C^+MHCII^+$ and was abrogated in cells isolated from NOSKO mice, suggesting that ACT-induced NOS2 activity contributed to the antitumor activity in myeloid cells. In addition to tumor killing properties, we also evaluated whether the transfer of $CD8^+$ T cells resulted in the antigen presentation activity of these cells inside the tumors. ACT triggered the ability of intra-tumoral $Ly6C^+MHCII^+$ cells to present antigen to naïve, OVA-specific $CD4^+$ T cells from OT-II transgenic mice (Figure 4C).

TNFα and NO production, coupled with the antigen presenting cell capacity, as well as cell surface marker profile (Figure 3B-3C) suggested that ACT caused the accumulation of an anti-tumor population of myeloid cells most similar to TNFα/iNOS producing, inflammatory ‘dendritic’ cells, often termed Tip-DCs (Aldridge et al., 2009; Serbina et al., 2003). We defined these cells as $CD11b^+$ $NOS2^+Ly6C^+MHCII^+$ and refer to them as Tip-DCs hereafter.

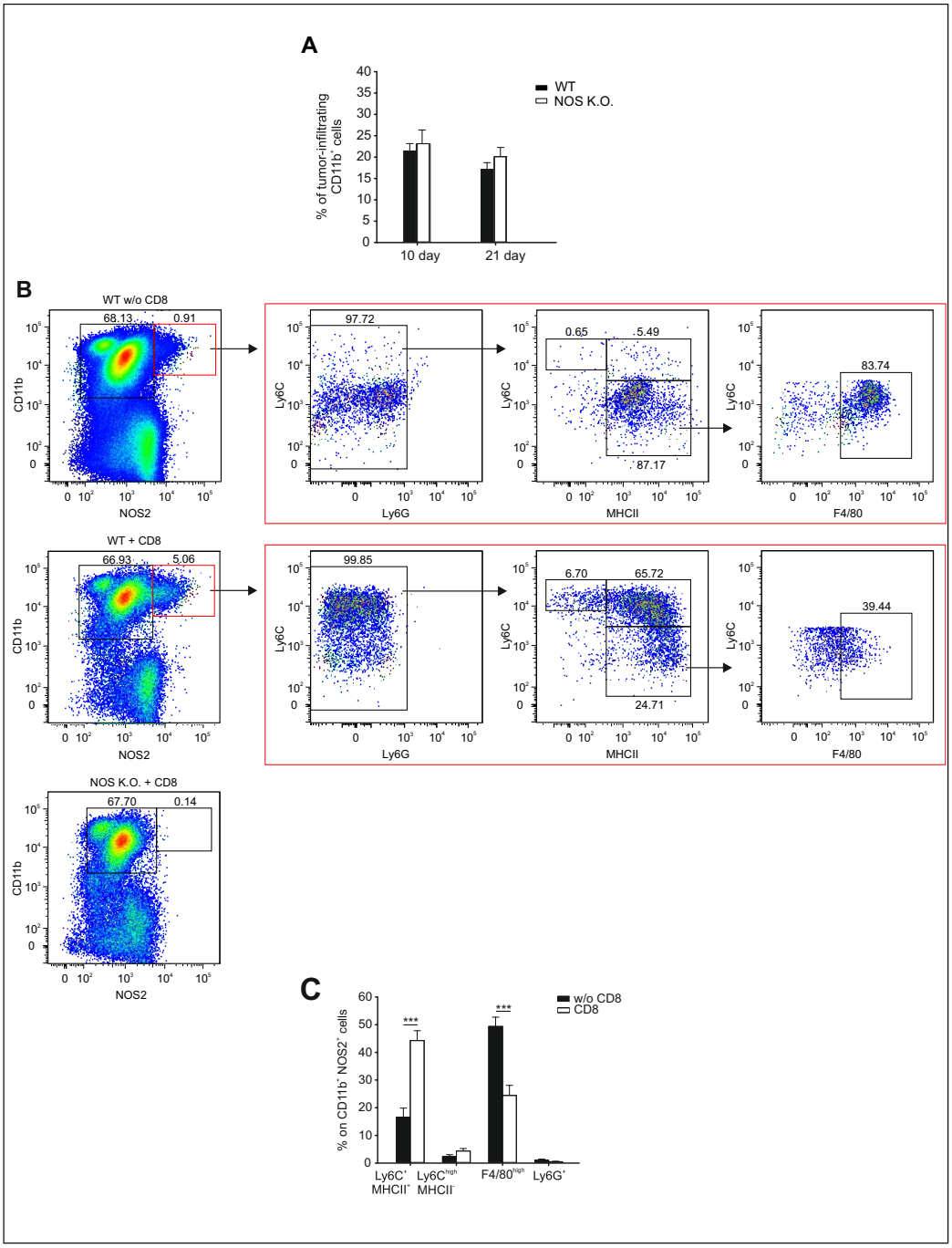

Figure 3. Flow cytometry analysis of myeloid sub-populations within tumor microenviroment
(A) Percentage of tumor-infiltrating $CD11b^{+}$cells in either WT or NOSKO mice at day 10 and 21 post-EG7 tumor implant. **(B)** Analysis of myeloid sub-populations in tumors treated with ACT. EG7 tumor-bearing, WT mice were either untreated (w/o CD8) or treated with ACT (CD8) and cells derived from tumors mass were used for analysis. Gating strategy for myeloid populations in $CD11b^{+}NOS2^{+}$ gate. NOSKO mice were used as a specificity control. **(C)** Quantification of different myeloid subpopulations in the $CD11b^{+}NOS2^{+}$ gate (N=18).

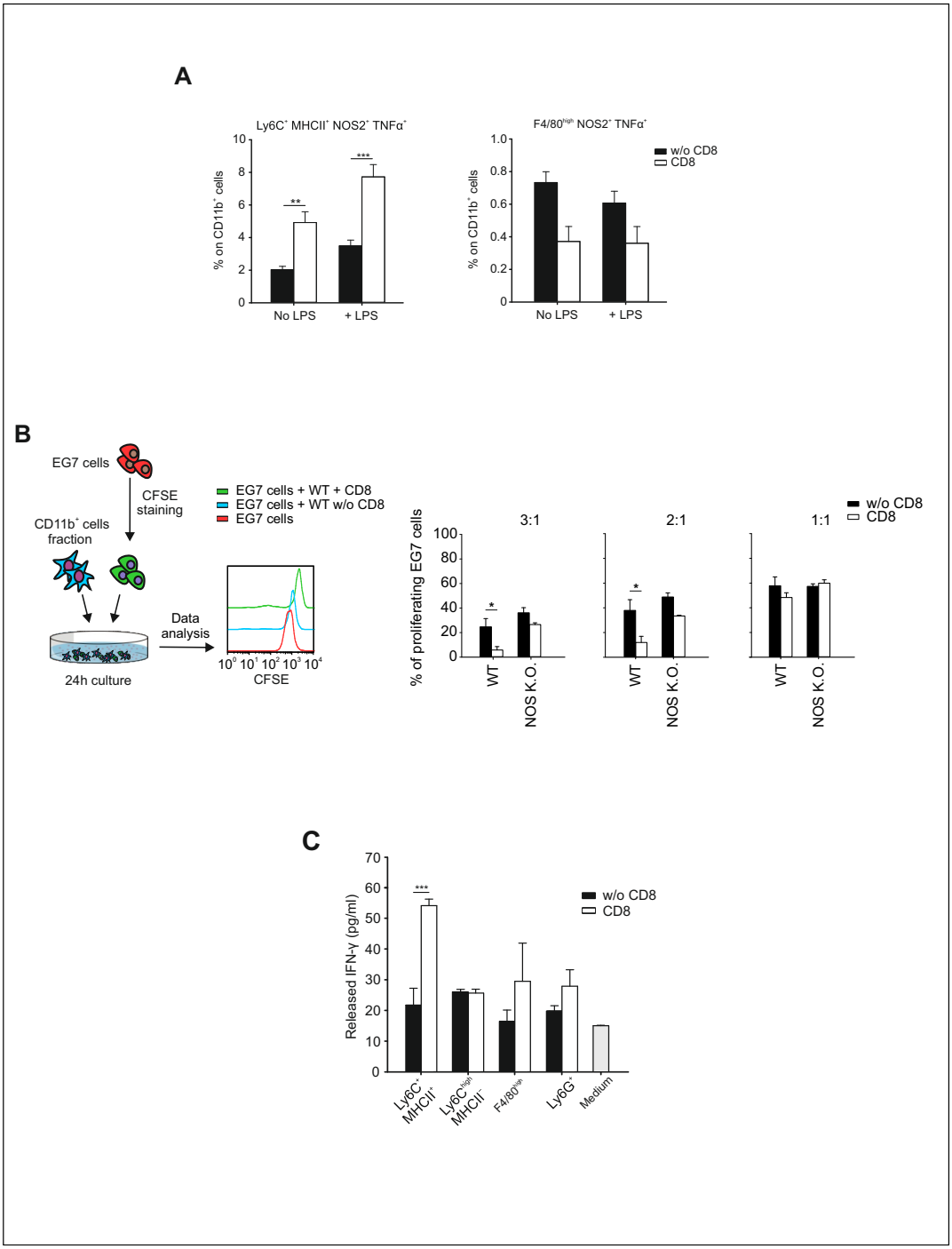

Figure 4. Tip-DCs activity

(A) Cell suspensions from tumors were stimulated or not with LPS; percentage of different myeloid subpopulations in CD11b$^+$ gate, (N=6).(B) Diagram indicates the overall experimental design to assess the proliferation of tumor cells. Ly6G$^-$CD11b$^+$ cells sorted from WT, NOSKO EG7-OVA tumor-bearing mice, either untreated or treated with ACT, co-cultured with CFSE-labeled EG7-OVA cells at the ratios (3:1, 2:1, 1:1). The percentage of proliferating EG7-OVA cells after co-culture compared to CFSE-labeled, EG7-OVA tumor cells cultured without Ly6G$^-$CD11b$^+$ cells is shown. Error bars, mean ± s.d, (n=9, pooled from 3 independent experiments); *p ≤0.05, unpaired Student t-test analysis. (C) Sorted myeloid subpopulations were cultured with naïve CD4$^+$ lymphocytes to evaluate IFN-γ released in supernatants.

Isolation of Tip-DCs and gene array characterization

After the phenotypic characterization of Tip-DC within tumor, we set up a protocol to isolate this population from tumors by fluorescence-activated cell sorting (*FACS*) using the NO fluorescent probe DAF-FM (Kojima et al., 1998). This probe is essentially no fluorescent until it reacts with NO to form fluorescent benzotriazole that can be detected with flow cytometry.

We sorted $CD11b^+$ $DAF\text{-}FM^+$ cells from WT tumors before and after ACT.

We observed, as we expected, an expansion on $CD11b^+$ $DAF\text{-}FM^+$ cells on tumors from mice treated with specific CD8+ T cells (Figure 5A), so we performed gene array characterization on sorted cells from WT tumors after immunotherapy (Figure 5B-E).

Our in-house Tip-DC samples were collected and merged with 3 publicly available datasets comprising microarray data of tissue macrophages (twelve samples), tissue dendritic cells (twelve samples), and monocytic myeloid-derived suppressor cells (nine samples). All data were measured on Affymetrix arrays and have been downloaded from Gene Expression Omnibus (http://www.ncbi.nlm.nih.gov/geo) or obtained by the authors of the original publications. Cluster and differential gene expression analysis was obtained using hierarchical clustering with Pearson correlation and centroid as distance metric and linkage, respectively.

The expression matrix of the myeloid cell collection were analysed with the Significance Analysis of Microarray method (SAM), coded in the samrRpackage (http://cran.rproject.org/web/packages/samr/index.html) to identify differentially expressed genes in the comparisons between subsets of macrophages, dendritic cells, and monocytic myeloid-derived suppressor cells (33 samples). These genes were identified using the multiclass procedure of sam Bioconductor package. The q-value threshold was set to 0, the contrast among the three classes was imposed to be different, and the SAM multiclass score was set ≥ 2. The multiclass analysis resulted in a list of 604 differentially expressed genes among macrophages, dendritic cells, and monocytic myeloid-derived suppressor cells.

We found that intra-tumoral Tip-DCs are transcriptionally more similar to tissue DCs (DCs) than to monocytic myeloid-derived suppressor cells (M-MDSC), or tissue macrophages (MFs). This similarity emerges using both a subset of genes differentially expressed between tissue MFs, tissue DCs and M-MDSCs, as well as a set of previously described gene signatures specific for DCs, macrophages and M-MDSCs.

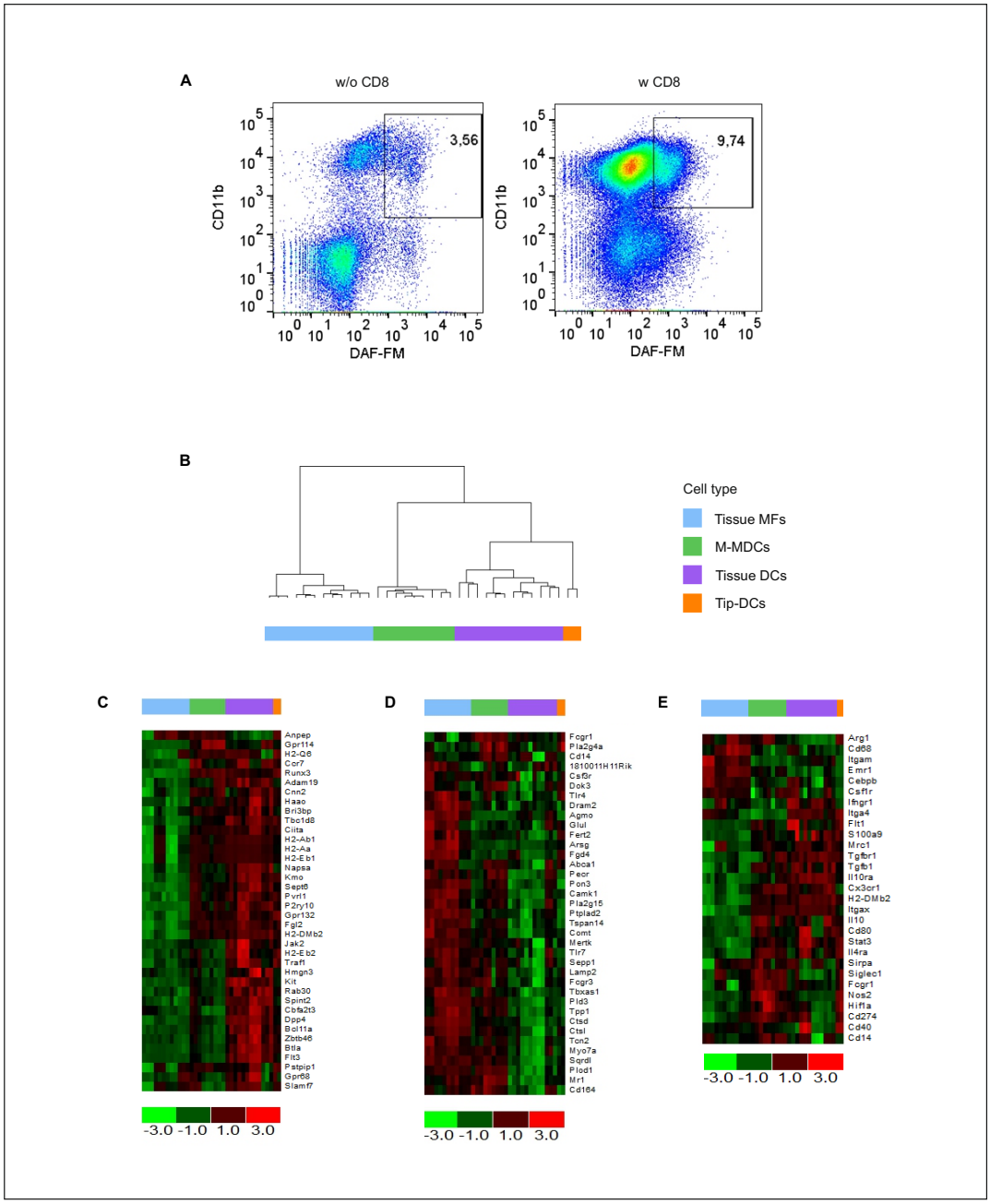

Figure 5. Tip-DCs isolation and supervised positioning of Tip-DCs
(A) Analysis of myeloid cells producing NO, from tumors challenged on wild type mice either treated with ACT or untreated. Tumor-infiltrating cells were loaded with DAF-FM for NO detection and labelled with CD11b antibody.**(B-E)** Gene expression profile analysis of the myeloid cell collection. An integrated gene expression matrix was generated merging transcriptional profiles of Tip-DCs and publicly available microarray data of tissue macrophages (MFs), tissue dendritic cells (DCs) and monocytic myeloid-derived suppressor cells (M-MDSCs). **(B)** Supervised positioning of Tip-DCs. Sample clustering using gene expression levels of 604 genes differentially expressed between tissue MFs, tissue DCs and M-MDSCs highlights that Tip-DCs are transcriptionally more similar to tissue DCs than to M-MDSCs or tissue macrophages.**(C)** Relative gene expression level of DC specific genes in tissue MFs, M-MDSCs, tissue DCs, and Tip-DCs. The heat map evidences that DC specific genes are expressed at comparable levels in both DCs and Tip-DCs, but not in tissue MFs and M-MDSCs. **(D)** Same as in (C) for macrophage specific genes**(E)** Same as in (C) for M-MDSC specific gene.

CD40-CD40L axis is required for Tip-DCs recruitment and tumor rejection after ACT

One important axis in the initiation and progression of cellular humoral and adoptive immunity is CD40-CD40L. Moreover, CD40 agonists induce T cell-dependent and independent tumor regression in both mice and patients with pancreatic cancer (Beatty et al., 2011). Also ligation of CD40 stimulates the induction of NOS2 in macrophages via an IFN-γ-dependent mechanism and it is therefore potentially important in activating NOS2 in the tumor microenvironment. We thus evaluated whether CD40-CD40L axis was necessary for NO-mediated immunotherapy. To investigate this issue, we stained viable slices from tumors grown in either CD40KO or CD40L KO mice.

We observed a significant reduction in NO release following interaction with tumor-specific $CD8^+$ T cells from OT-1, on CD40L KO compared to WT mice, thus suggesting a role of CD40/CD40L axis on tissue-infiltrating cells to sustain NOS2 activation with prevalent role for host CD40L expression (Figure 6A-B). To clarify further the role of CD40L expression in the NO induction, we performed NO imaging experiments on viable tumor slices from either WT or CD40L KO mice, by using polyclonal OVA-specific $CD8^+$ T cells expanded from the spleens of either WT or CD40L KO mice (Figure 7A-B). Our data indicated that the greatest reduction in NO release was observed when CD40L-deficient OVA-specific lymphocytes were added to CD40L KO tumor slices.

To confirm the specificity of the CD40-CD40L axis in tumor rejection, we performed ACT in CD40 KO and CD40L KO mice bearing EG7 tumors and we monitored the survival following ACT (Figure 7C). We found that lack of CD40L completely abrogated the therapeutic effect while lack of CD40 induced a partial benefit. The differences between the phenotypes of the receptor and ligand deficiencies are likely attributed to the fact that CD40 only binds CD40L, while CD40L has at least two other integrin binding partners that extend its range of actions. These findings clearly confirm the involvement of CD40-CD40L axis on ACT effectiveness.

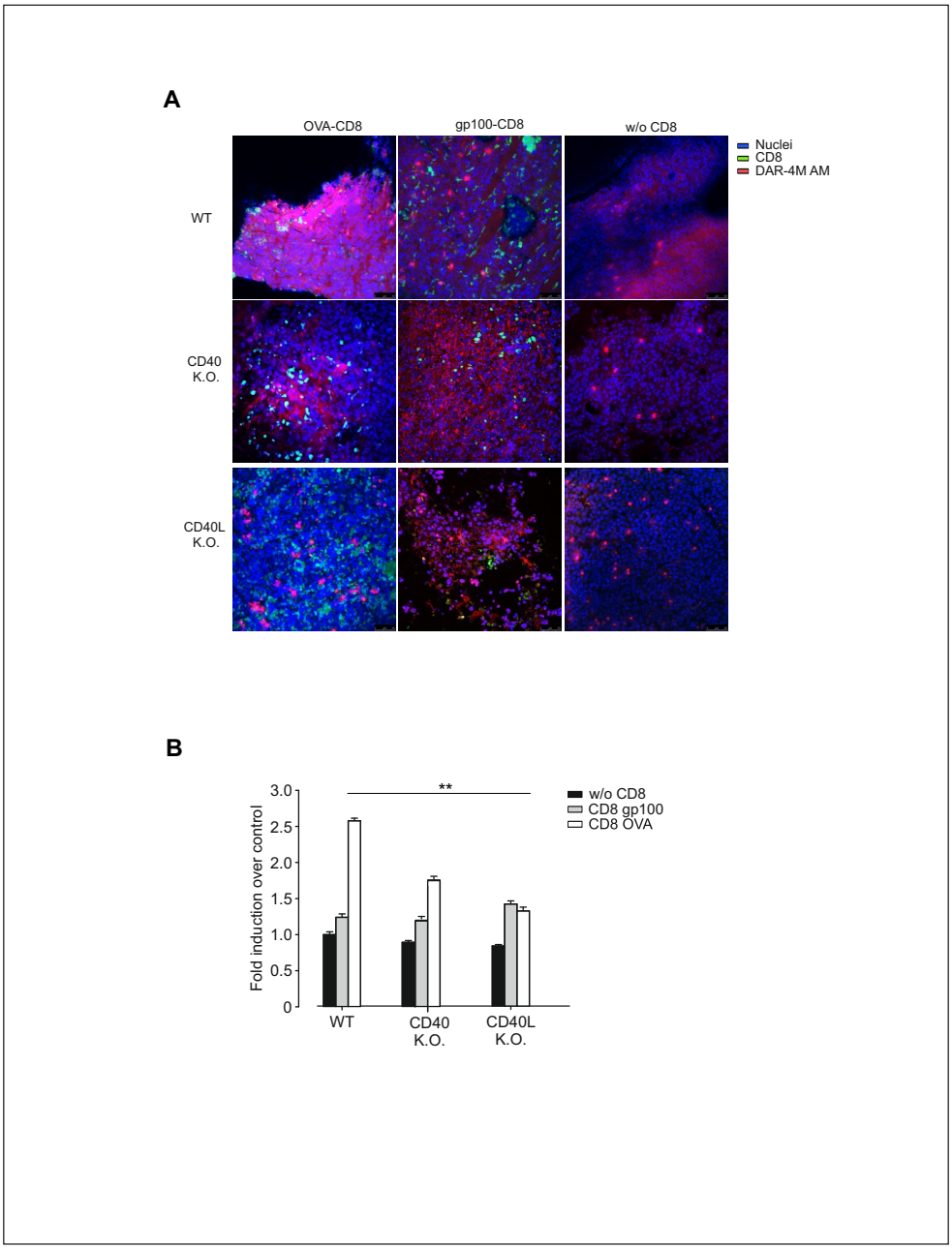

Figure 6. CD40-CD40L is necessary for NO induction after T cell interaction
(A) Representative images of NO production after T cell interaction within viable tumor slices. From the left: NO production (red) in the presence of OVA-specific $CD8^+$ T cells (green, OVA-CD8), gp100-specific $CD8^+$ T cells (green, gp100-CD8) or in the absence of $CD8^+$ T cells (w/o CD8). Top: tumor slices from WT mice; center: tumor slices from CD40KO; bottom: tumor slices from CD40L KO mice. DAPI (blue). Scale bar, 50 µm. **(B)** Released NO levels were measured as mean of fluorescence expressed as fold induction over the control (w/o CD8). Error bars, mean ± s.e.m. ; (n=12, pooled from 3 independent experiments), *** $p \leq 0.001$, unpaired Student t-test analysis.

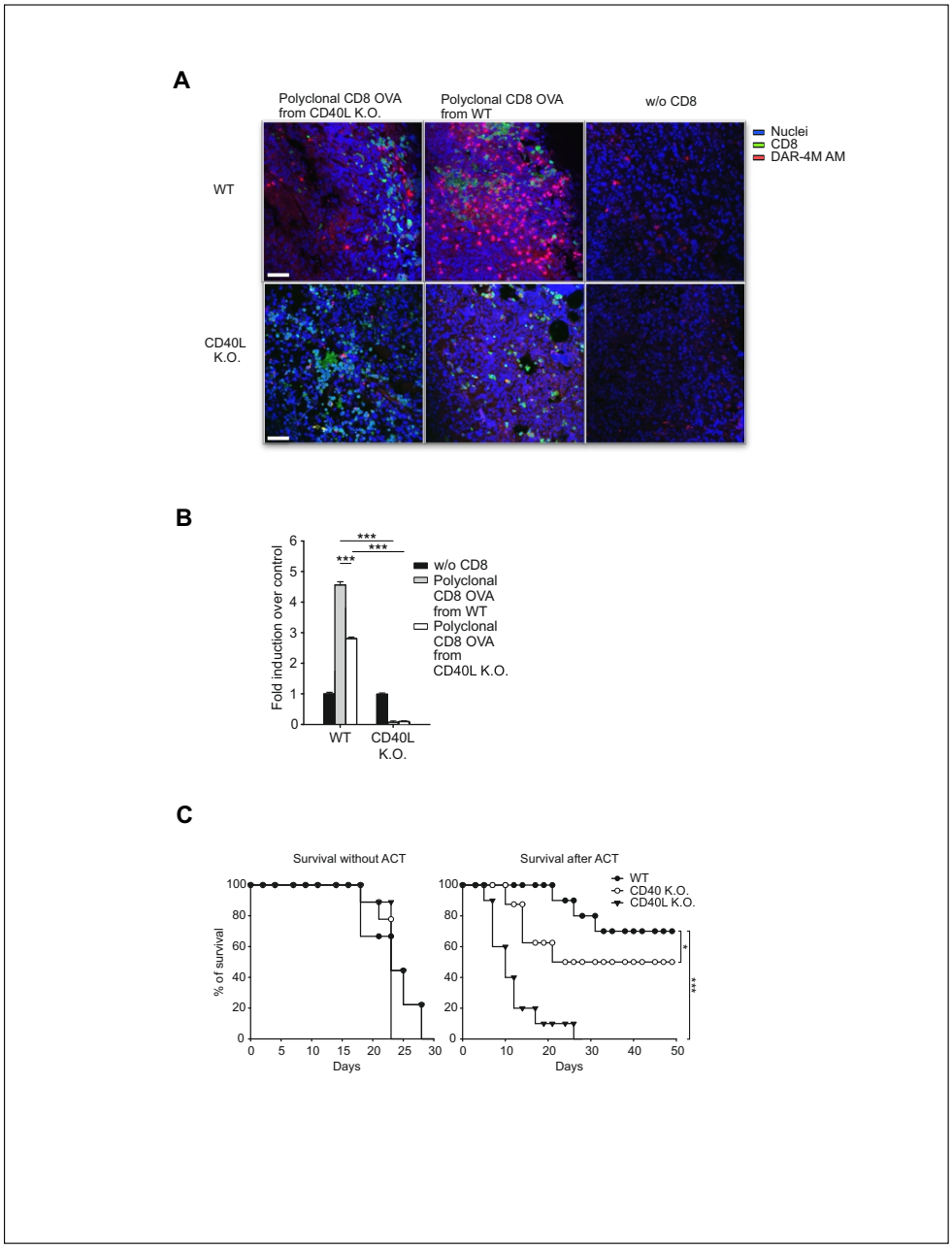

Figure 7. CD40/CD40L is necessary for NO induction and ACT effectiveness
(A) Representative images of NO production after T cell interaction within viable tumor slices. CFSE-labeled, polyclonal $CD8^+$ T cells specific for OVA were derived from immunized WT or E8IcreXCD40L$^{flox/flox}$ mice and were incubated with EG7 tumor slices from either WT or CD40L K.O. mice from the left: NO production (red) in the presence of polyclonal OVA-specific CD8 cells from WT mice (green, polyclonal OVA-CD8 from WT), polyclonal OVA-specific $CD8^+$ cells from CD40L K.O. mice (green, polyclonal CD8-OVA from K.O.) or in the absence of $CD8^+$ T cells (w/o CD8). Top: tumor slices from WT mice; bottom: tumor slices from CD40L K.O. mice. DAPI (blue). Scale bar, 50 µm. (B) Released NO levels were measured as mean of fluorescence expressed as fold induction over the control (w/o CD8). Error bars, mean ± s.e.m. ; (n=12, pooled from 3 independent experiments), *** p ≤0.001, unpaired Student t-test analysis. (C) Survival percentages of WT, CD40 K.O. and CD40L K.O., EG7 tumor-bearing mice either untreated (left) or undergoing ACT (right, *n*=10, mice/group). *P≤0.05 *** p≤0.001, log-rank test.

Discussion

The success of ACT - based on the infusion of *ex vivo* expanded tumor infiltrating lymphocytes (TILs)- is limited by crucial events as the trafficking of adoptively transferred cells to the tumor site (Melero et al., 2014b) and the highly immunosuppressive environment of developing cancer (Shiao et al., 2011).

At the tumor site, immunosuppressive functions are exerted by distinct cell populations as MDSCs and TAMs, that are known to suppress T cell proliferation through several direct and indirect mechanisms (Ugel et al., 2015). A master event, regulating T cell functionality within tumors, is the alteration of arginine metabolism, which is mainly caused by the selective up regulation of ARG1 and NOS2 enzymes within malignant tissues. (Gabrilovich et al., 2012; Marigo et al., 2010). Evidence from animal models and humans indicates that L-arginine metabolism is important in physiological, as well as pathological, conditions (Gabrilovich et al., 2012). Nonetheless, the precise role of ARG1 and NOS2 and their products in cancer remains controversial.

Indeed, increased NOS2 expression in breast cancer patients is associated with poor clinical outcome and decreased survival (Glynn et al., 2010). On the other hand, in some human carcinomas the increment of NOS2 correlates with higher infiltration of $CD4^+$ and $CD8^+$ T cells after therapy (Klug et al., 2013). The relative role of NOS2 mainly relies on the cell types up-regulating the expression of this enzyme and the relative NO concentration within the tumor microenvironment.

Effectively, NO may promote tumor progression and metastasis by the direct induction of tumor-cell proliferation, migration and invasion, and indirectly through the expression of angiogenic and lymphangiogenic factors in tumor cells at low concentration. On the other hand, high doses of NO have cytotoxic effects, which can result in tumor regression and metastasis inhibition (Fukumura et al., 2006).

In line with our previous investigations, we would have expected an improvement of ACT in tumor-bearing hosts in which the NOS2 enzyme was totally ablated. Interestingly, we found that NOS2 was necessary for the effectiveness of ACT, since we observed that the lack of this enzyme increased the number and activity of $CD8^+$T cells. The failure of immunotherapy in NOSKO was totally unexpected for the well-known suppressive role of NOS2. Our results so far opened a more intricate *scenarium* with new questions to be addressed: why and how NOS2 is necessary for the effectiveness of ACT? Does nitric oxide play a key role in T cell activity within the tumor microenvironment?

In order to address these questions, we started by monitoring NO dynamics at the tumor site after the addition of tumor specific T lymphocytes. To this aim, we developed a new method to detect in real-time NO production and release within viable tumor slices. The technical advantage of this approach is the use of the fluorescent probe diaminorhodamine (DAR 4M –AM), which specifically reacts with NO over other potentially interfering molecules, in combination with confocal microscopy. On the contrary, the conventional methods applied for NO tracking, such as chemiluminescence and spectroscopy, required complicated instrumentation and additionally they suffered from low spatial resolution tracking (Lim, Xu et al. 2006).

Our data clearly demonstrated that antigen-specific T cells are able to trigger NO release within the tumor microenvironment. Importantly, we observed an impairment of NO after antigen specific T cell addition underlining that NO is mainly produced by NOS2 activity in the tumor mass.

After the awareness that NOS2 and NO are required to sustain tumor rejection, we focused our attention on which cell population could be responsible of its generation at the tumor site. It is known that NO is a key regulator of myeloid inflammatory cells and its production was reported from macrophages but it is still debated whether it can also be originated from other immune cell subsets, as mast cells and dendritic cells (Predonzani et al., 2015).
Indeed, we first analyzed the myeloid compartment in tumors before and after ACT. When we analyzed the entire myeloid cell population in tumors, we did not find any significant differences in the total $CD11b^+$ cell percentage before and after ACT. So, we analyzed the distribution of distinct myeloid subsets within the tumor microenvironment before and after ACT.
Indeed, after ACT, we observed an expansion of a specific population, $CD11b^+NOS2^+$ $Ly6C^+MHCII^{++}$cells, which was absent in NOSKO mice and wild type mice without treatment. Moreover, the lack of F4/80 in this population, a specific marker of macrophages, together with the decrement of macrophage percentage in tumors after ACT, suggested that they are not responsible for NO generation at the tumor site. Additionally, the lack of the $CD11b^+NOS2^+$ $Ly6C^+MHCII^{++}$cell subset in either untreated (no ACT) or NOSKO mice suggested that ACT was able to induce the up regulation of NOS2 thus triggering NO generation, which in turn promotes the reduction of macrophages ($F4/80^+$ cells) with a parallel increment of this new subset of cells within the tumor microenvironment.

Evidence from our *in vivo* and *in vitro* experiments highlighted the anti-tumor nature of this newly identified cell subset. This was further confirmed by functional assays, showing the ability of this cell population to secrete TNFα after stimulation with LPS and their cytostatic ability against tumors cells. Further confirmation of the anti-tumor activity of this subset came from their ability to cross-present, antigens, which is crucial for the generation of effector $CD8^+$ T cell response (Fehres et al., 2014). Essentially, all the functional assays performed underlined that antitumor activities were exclusive of $CD11b^+NOS2^+Ly6C^+MHCII^+$ cells and were enhanced after ACT protocols.
The immune phenotype, the functional abilities and in particular NO generation observed within viable tumor slices, suggested that this intratumoral myeloid population, expanded after ACT, closely resembled the TNF/iNOS producing dendritic cells also known as Tip-DC, identified under inflammatory conditions or infections. Interestingly, the main roles attributed to Tip-DCs are: i) the rapid and local activation of T cell responses, for example for the resolution of infection(Aldridge et al., 2009; Serbina et al., 2003) and ii) the pro-inflammatory activity in psoriatic lesions of patients skin (Chong et al., 2011; Lowes et al., 2005). A key feature of Tip-DCs is their ability to prime naïve T cells. To further characterize the identity of this cell subset, we isolated this population from tumors by means of their ability to generate NO. Indeed, we set-up a FACS

sorting strategy based on a NO-specific fluorescent probe DAF-FM, an analogue of DAR 4M AM, which is more suitable for the flow cytometry approach.
Indeed, we isolated $CD11b^+$ $DAF\text{-}FM^+$ cells from wild type tumors before and after ACT, and we subsequently performed gene array profiling on sorted myeloid cell subsets. The gene array characterization was performed merging our in-house Tip-DC with 3 publicly available datasets comprising microarray data of tissue macrophages (twelve samples), tissue dendritic cells (twelve samples), and monocytic myeloid-derived suppressor cells (nine samples). All data were measured on Affymetrix arrays and have been downloaded from Gene Expression Omnibus (http://www.ncbi.nlm.nih.gov/geo) or obtained by the authors of the original publications. We found that this intratumoral myeloid population - expanded after ACT and identified as TNF/iNOS producing cells - was transcriptionally more similar to tissue DCs (DCs) than to monocytic myeloid-derived suppressor cells (M-MDSC), or tissue macrophages (MFs). This similarity emerges using both a subset of genes differentially expressed between tissue MFs, tissue DCs and M-MDSCs, as well as a set of previously described gene signatures specific for DCs, macrophages and M-MDSCs. Indeed, the transcriptional correspondence emerged between our cells and inflammatory dendritic cells together with their functional activities and immune phenotype, allowed us to identify without any doubts this population as Tip-DCs.

Importantly, our study for the first time described and characterized Tip-DCs within the tumor microenvironment. Indeed, our data indicated that Tip-DCs beyond the control of infections play additional immune functions as the control of tumor growth in the ACT setting.
The identification and expansion of Tip-DCs in tumors opened important questions for cancer immunotherapy: i) how are Tip-DCs involved on tumor rejection? ii) how are these cells recruited within the tumor microenvironment? iii) are there any possible uses of these cells to improve the outcome of cancer immunotherapy?

Considering our results, it is clear that ACT requires the triggering of an intra-tumoral, virtuous circle where $CD8^+$ T cell recognition of tumor antigen is necessary to recruit Tip-DCs and activate them to present tumor antigens, further promoting T cell expansion, and trigger their killing activity by TNFα and NO production. A role for NO production in the efficacy of ACT for the treatment of skin cancer was previously suggested (Miguel et al., 2010), but in that context, the production of NO was attributed to macrophages, which was excluded in our settings. Notwithstanding, the crucial event regulating Tip-DC expansion in tumors is the cross talk between these cells and antigen specific T CD8+ lymphocytes. Indeed, we investigated the specific mechanism underpinning these dynamic interactions.

To this aim, we first analysed the CD40-CD40L axis, since it controls an array of pathways at the base of both initiation and progression of cellular and humoral adaptive immunity (Summers deLuca et al., 2011). Moreover, CD40 agonists induce T cell-dependent and independent tumor regressions in both mice and patients with pancreatic cancer (Beatty et al., 2011). Thus, we analysed viable tumor slices either from CD40L KO mice or CD40KO mice. We observed a

reduction of NO induction on viable slices derived from CD40LKO mice compared to the controls. The engagement of CD40-CD40L axis behind NO-mediated therapy exerted by Tip-DCs was also confirmed by our *in vitro* experiments. Interestingly, our data obtained on viable tumor slices by using polyclonal OVA-specific $CD8^+$ T cells expanded from CD40L KO mice, suggested that CD40L was provided by tumor infiltrating $CD8^+$ T lymphocytes. Finally, our *in vivo* data showed clearly the involvement of CD40-CD40L axis on ACT effectiveness. Indeed we found that the lack of CD40L completely abrogated the therapeutic effect while lack of CD40 induced a partial benefit in ACT protocols.
Our data clearly demonstrated an involvement of this axis on NO-mediated tumor rejection. In fact, the controversial results of CD40 could be ascribed to the fact that CD40 only binds CD40L, while CD40L has at least two other integrin binding partners that extend its range of actions (Alaaeddine et al., 2011) . Certainly these mechanism needs to be clarify in details with more investigation; at the moment, we first identified CD40-CD40L as key pathway in governing the interplay between therapeutic anti-cancer T cells and the local immunosuppressive microenvironment.

In conclusion, in this study we proposed a new approach to study NO dynamics within the tumor microenvironment based on both confocal microscopy and flow cytometry. Thanks to this technological advances, we characterized for the first time in tumors a new subset of myeloid cells named Tip-DCs, endorsed with anti-tumor activity, which can be potentially exploited to improve cancer immunotherapy. Most significantly, we shed light on new mechanisms regulating activated T -myeloid cell interactions occurring at the tumor microenvironment. Remarkably, we pointed out NOS2 and NO as principal effectors of tumor killing in ACT protocols.
Our study brought the awareness that NOS2 is fundamental for the effectiveness of ACT, opening new perspectives to improve cancer immunotherapy based on NOS2/NO modulation in tumors.

References

Alaaeddine, N., Hassan, G.S., Yacoub, D., Mourad, W., Alaaeddine, N., Hassan, G.S., Yacoub, D., and Mourad, W. (2011). CD154: An Immunoinflammatory Mediator in Systemic Lupus Erythematosus and Rheumatoid Arthritis. J. Immunol. Res. J. Immunol. Res. 2012, 2012, e490148.

Alderton, W.K., Cooper, C.E., and Knowles, R.G. (2001). Nitric oxide synthases: structure, function and inhibition. Biochem. J. 357, 593–615.

Aldridge, J.R., Moseley, C.E., Boltz, D.A., Negovetich, N.J., Reynolds, C., Franks, J., Brown, S.A., Doherty, P.C., Webster, R.G., and Thomas, P.G. (2009). TNF/iNOS-producing dendritic cells are the necessary evil of lethal influenza virus infection. Proc. Natl. Acad. Sci. U. S. A. 106, 5306–5311.

Banchereau, J., Bazan, F., Blanchard, D., Brière, F., Galizzi, J.P., van Kooten, C., Liu, Y.J., Rousset, F., and Saeland, S. (1994). The CD40 antigen and its ligand. Annu. Rev. Immunol. 12, 881–922.

Beatty, G.L., Chiorean, E.G., Fishman, M.P., Saboury, B., Teitelbaum, U.R., Sun, W., Huhn, R.D., Song, W., Li, D., Sharp, L.L., et al. (2011). CD40 Agonists Alter Tumor Stroma and Show Efficacy Against Pancreatic Carcinoma in Mice and Humans. Science 331, 1612–1616.

Belz, G.T., and Nutt, S.L. (2012). Transcriptional programming of the dendritic cell network. Nat. Rev. Immunol. 12, 101–113.

Besser, M.J., Shapira-Frommer, R., Treves, A.J., Zippel, D., Itzhaki, O., Hershkovitz, L., Levy, D., Kubi, A., Hovav, E., Chermoshniuk, N., et al. (2010). Clinical responses in a phase II study using adoptive transfer of short-term cultured tumor infiltration lymphocytes in metastatic melanoma patients. Clin. Cancer Res. Off. J. Am. Assoc. Cancer Res. 16, 2646–2655.

Bingisser, R.M., Tilbrook, P.A., Holt, P.G., and Kees, U.R. (1998). Macrophage-Derived Nitric Oxide Regulates T Cell Activation via Reversible Disruption of the Jak3/STAT5 Signaling Pathway. J. Immunol. 160, 5729–5734.

Biswas, S.K., and Mantovani, A. (2010). Macrophage plasticity and interaction with lymphocyte subsets: cancer as a paradigm. Nat. Immunol. 11, 889–896.

Bonavida, B. (2010). Nitric Oxide (NO) and Cancer: Prognosis, Prevention, and Therapy (Springer Science & Business Media).

Bosschaerts, T., Guilliams, M., Stijlemans, B., Morias, Y., Engel, D., Tacke, F., Hérin, M., De Baetselier, P., and Beschin, A. (2010). Tip-DC Development during Parasitic Infection Is Regulated by IL-10 and Requires CCL2/CCR2, IFN-γ and MyD88 Signaling. PLoS Pathog 6, e1001045.

Bryan, N.S., and Grisham, M.B. (2007). Methods to detect nitric oxide and its metabolites in biological samples. Free Radic. Biol. Med. 43, 645–657.

Burke, A.J., Sullivan, F.J., Giles, F.J., and Glynn, S.A. (2013). The yin and yang of nitric oxide in cancer progression. Carcinogenesis 34, 503–512.

Carmeliet, P., and Jain, R.K. (2011). Molecular mechanisms and clinical applications of angiogenesis. Nature 473, 298–307.

Caux, C., Massacrier, C., Vanbervliet, B., Dubois, B., Van Kooten, C., Durand, I., and Banchereau, J. (1994). Activation of human dendritic cells through CD40 cross-linking. J. Exp. Med. 180, 1263–1272.

Chao, J.-I., Kuo, P.-C., and Hsu, T.-S. (2004). Down-regulation of survivin in nitric oxide-induced cell growth inhibition and apoptosis of the human lung carcinoma cells. J. Biol. Chem. 279, 20267–20276.

Chong, S.Z., Wong, K.L., Lin, G., Yang, C.M., Wong, S.-C., Angeli, V., Macary, P.A., and Kemeny, D.M. (2011). Human $CD8^+$ T cells drive Th1 responses through the differentiation of TNF/iNOS-producing dendritic cells. Eur. J. Immunol. 41, 1639–1651.

Coleman, J.W. (2001). Nitric oxide in immunity and inflammation. Int. Immunopharmacol. 1, 1397–1406.

Doorbar, J. (2006). Molecular biology of human papillomavirus infection and cervical cancer. Clin. Sci. Lond. Engl. 1979 110, 525–541.

Dudley, M.E., Wunderlich, J.R., Yang, J.C., Sherry, R.M., Topalian, S.L., Restifo, N.P., Royal, R.E., Kammula, U., White, D.E., Mavroukakis, S.A., et al. (2005). Adoptive cell transfer therapy following non-myeloablative but lymphodepleting chemotherapy for the treatment of patients with refractory metastatic melanoma. J. Clin. Oncol. Off. J. Am. Soc. Clin. Oncol. 23, 2346–2357.

DuPage, M., Mazumdar, C., Schmidt, L.M., Cheung, A.F., and Jacks, T. (2012). Expression of tumour-specific antigens underlies cancer immunoediting. Nature 482, 405–409.

Essand, M., and Loskog, A.S.I. (2013). Genetically engineered T cells for the treatment of cancer. J. Intern. Med. 273, 166–181.

van Essen, D., Kikutani, H., and Gray, D. (1995). CD40 ligand-transduced co-stimulation of T cells in the development of helper function. Nature 378, 620–623.

Farias-Eisner, R., Sherman, M.P., Aeberhard, E., and Chaudhuri, G. (1994). Nitric oxide is an important mediator for tumoricidal activity in vivo. Proc. Natl. Acad. Sci. U. S. A. 91, 9407–9411.

Fehres, C.M., Unger, W.W.J., Garcia-Vallejo, J.J., and van Kooyk, Y. (2014). Understanding the biology of antigen cross-presentation for the design of vaccines against cancer. Antigen Present. Cell Biol. 5, 149.

Fernandez, N.C., Lozier, A., Flament, C., Ricciardi-Castagnoli, P., Bellet, D., Suter, M., Perricaudet, M., Tursz, T., Maraskovsky, E., and Zitvogel, L. (1999). Dendritic cells directly trigger NK cell functions: cross-talk relevant in innate anti-tumor immune responses in vivo. Nat. Med. 5, 405–411.

Finn, O.J. (2003). Cancer vaccines: between the idea and the reality. Nat. Rev. Immunol. 3, 630–641.

Franchi, A., Massi, D., Santucci, M., Masini, E., Rossi Degl'Innocenti, D., Magnelli, L., Fanti, E., Naldini, A., Ardinghi, C., Carraro, F., et al. (2006). Inducible nitric oxide synthase activity correlates with lymphangiogenesis and vascular endothelial growth factor-C expression in head and neck squamous cell carcinoma. J. Pathol. 208, 439–445.

Fridlender, Z.G., Sun, J., Kim, S., Kapoor, V., Cheng, G., Ling, L., Worthen, G.S., and Albelda, S.M. (2009). Polarization of tumor-associated neutrophil phenotype by TGF-beta: "N1" versus "N2" TAN. Cancer Cell 16, 183–194.

Fukumura, D., Kashiwagi, S., and Jain, R.K. (2006). The role of nitric oxide in tumour progression. Nat. Rev. Cancer 6, 521–534.

Gabrilovich, D. (2004). Mechanisms and functional significance of tumour-induced dendritic-cell defects. Nat. Rev. Immunol. 4, 941–952.

Gabrilovich, D.I., Ostrand-Rosenberg, S., and Bronte, V. (2012). Coordinated regulation of myeloid cells by tumours. Nat. Rev. Immunol. 12, 253–268.

Gajewski, T.F., Schreiber, H., and Fu, Y.-X. (2013). Innate and adaptive immune cells in the tumor microenvironment. Nat. Immunol. 14, 1014–1022.

Galon, J., Pagès, F., Marincola, F.M., Angell, H.K., Thurin, M., Lugli, A., Zlobec, I., Berger, A., Bifulco, C., Botti, G., et al. (2012). Cancer classification using the Immunoscore: a worldwide task force. J. Transl. Med. 10, 205.

Ghafourifar, P., and Cadenas, E. (2005). Mitochondrial nitric oxide synthase. Trends Pharmacol. Sci. 26, 190–195.

Glynn, S.A., Boersma, B.J., Dorsey, T.H., Yi, M., Yfantis, H.G., Ridnour, L.A., Martin, D.N., Switzer, C.H., Hudson, R.S., Wink, D.A., et al. (2010). Increased NOS2 predicts poor survival in estrogen receptor-negative breast cancer patients. J. Clin. Invest. 120, 3843–3854.

Goc, J., Germain, C., Vo-Bourgais, T.K.D., Lupo, A., Klein, C., Knockaert, S., de Chaisemartin, L., Ouakrim, H., Becht, E., Alifano, M., et al. (2014). Dendritic cells in tumor-associated tertiary lymphoid structures signal a Th1 cytotoxic immune contexture and license the positive prognostic value of infiltrating CD8+ T cells. Cancer Res. 74, 705–715.

Grewal, I.S., Xu, J., and Flavell, R.A. (1995). Impairment of antigen-specific T-cell priming in mice lacking CD40 ligand. Nature 378, 617–620.

Grewal, I.S., Foellmer, H.G., Grewal, K.D., Xu, J., Hardardottir, F., Baron, J.L., Janeway, C.A., and Flavell, R.A. (1996). Requirement for CD40 ligand in costimulation induction, T cell activation, and experimental allergic encephalomyelitis. Science 273, 1864–1867.

Grisham, M.B., Johnson, G.G., and Lancaster, J.R. (1996). Quantitation of nitrate and nitrite in extracellular fluids. Methods Enzymol. 268, 237–246.

Guo, C., Manjili, M.H., Subjeck, J.R., Sarkar, D., Fisher, P.B., and Wang, X.-Y. (2013). Chapter Seven - Therapeutic Cancer Vaccines: Past, Present, and Future. In Advances in Cancer Research, K.D.T. and P.B. Fisher, ed. (Academic Press), pp. 421–475.

Habib, S., and Ali, A. (2011). Biochemistry of Nitric Oxide. Indian J. Clin. Biochem. 26, 3–17.

Hall, C.N., and Garthwaite, J. (2009). What is the real physiological NO concentration in vivo? Nitric Oxide Biol. Chem. Off. J. Nitric Oxide Soc. 21, 92–103.

Hall, A.V., Antoniou, H., Wang, Y., Cheung, A.H., Arbus, A.M., Olson, S.L., Lu, W.C., Kau, C.L., and Marsden, P.A. (1994). Structural organization of the human neuronal nitric oxide synthase gene (NOS1). J. Biol. Chem. 269, 33082–33090.

Hanahan, D., and Weinberg, R.A. (2011). Hallmarks of cancer: the next generation. Cell 144, 646–674.

Hodi, F.S., O'Day, S.J., McDermott, D.F., Weber, R.W., Sosman, J.A., Haanen, J.B., Gonzalez, R., Robert, C., Schadendorf, D., Hassel, J.C., et al. (2010). Improved Survival with Ipilimumab in Patients with Metastatic Melanoma. N. Engl. J. Med. 363, 711–723.

Hudis, C.A. (2007). Trastuzumab — Mechanism of Action and Use in Clinical Practice. N. Engl. J. Med. 357, 39–51.

Humphries, C. (2013). Adoptive cell therapy: Honing that killer instinct. Nature 504, S13–S15.

Itoh, Y., Ma, F.H., Hoshi, H., Oka, M., Noda, K., Ukai, Y., Kojima, H., Nagano, T., and Toda, N. (2000). Determination and bioimaging method for nitric oxide in biological specimens by diaminofluorescein fluorometry. Anal. Biochem. 287, 203–209.

Itzhaki, O., Hovav, E., Ziporen, Y., Levy, D., Kubi, A., Zikich, D., Hershkovitz, L., Treves, A.J., Shalmon, B., Zippel, D., et al. (2011). Establishment and large-scale expansion of minimally cultured "young" tumor infiltrating lymphocytes for adoptive transfer therapy. J. Immunother. Hagerstown Md 1997 34, 212–220.

Jain, R.K. (2005). Normalization of tumor vasculature: an emerging concept in antiangiogenic therapy. Science 307, 58–62.

Janssens, S.P., Shimouchi, A., Quertermous, T., Bloch, D.B., and Bloch, K.D. (1992). Cloning and expression of a cDNA encoding human endothelium-derived relaxing factor/nitric oxide synthase. J. Biol. Chem. 267, 14519–14522.

Kantoff, P.W., Higano, C.S., Shore, N.D., Berger, E.R., Small, E.J., Penson, D.F., Redfern, C.H., Ferrari, A.C., Dreicer, R., Sims, R.B., et al. (2010a). Sipuleucel-T immunotherapy for castration-resistant prostate cancer. N. Engl. J. Med. 363, 411–422.

Kantoff, P.W., Schuetz, T.J., Blumenstein, B.A., Glode, L.M., Bilhartz, D.L., Wyand, M., Manson, K., Panicali, D.L., Laus, R., Schlom, J., et al. (2010b). Overall survival analysis of a phase II randomized controlled trial of a Poxviral-based PSA-targeted immunotherapy in metastatic castration-resistant prostate cancer. J. Clin. Oncol. Off. J. Am. Soc. Clin. Oncol. 28, 1099–1105.

Katsnelson, A. (2006). Kicking off adaptive immunity: the discovery of dendritic cells. J. Exp. Med. 203, 1622.

Kelleher, M., and Beverley, P.C. (2001). Lipopolysaccharide modulation of dendritic cells is insufficient to mature dendritic cells to generate CTLs from naive polyclonal CD8+ T cells in vitro, whereas CD40 ligation is essential. J. Immunol. Baltim. Md 1950 167, 6247–6255.

Khong, A., Nelson, D.J., Nowak, A.K., Lake, R.A., and Robinson, B.W.S. (2012). The use of agonistic anti-CD40 therapy in treatments for cancer. Int. Rev. Immunol. 31, 246–266.

Klug, F., Prakash, H., Huber, P.E., Seibel, T., Bender, N., Halama, N., Pfirschke, C., Voss, R.H., Timke, C., Umansky, L., et al. (2013). Low-dose irradiation programs macrophage differentiation to an iNOS$^+$/M1 phenotype that orchestrates effective T cell immunotherapy. Cancer Cell 24, 589–602.

Kochenderfer, J.N., Wilson, W.H., Janik, J.E., Dudley, M.E., Stetler-Stevenson, M., Feldman, S.A., Maric, I., Raffeld, M., Nathan, D.-A.N., Lanier, B.J., et al. (2010). Eradication of B-lineage cells and regression of lymphoma in a patient treated with autologous T cells genetically engineered to recognize CD19. Blood 116, 4099–4102.

Kojima, H., Nakatsubo, N., Kikuchi, K., Kawahara, S., Kirino, Y., Nagoshi, H., Hirata, Y., and Nagano, T. (1998). Detection and imaging of nitric oxide with novel fluorescent indicators: diaminofluoresceins. Anal. Chem. 70, 2446–2453.

Leon, L., Jeannin, J.-F., and Bettaieb, A. (2008). Post-translational modifications induced by nitric oxide (NO): implication in cancer cells apoptosis. Nitric Oxide Biol. Chem. Off. J. Nitric Oxide Soc. 19, 77–83.

Li, H., and Wan, A. (2015). Fluorescent probes for real-time measurement of nitric oxide in living cells. The Analyst 140, 7129–7141.

Lim, M.H. (2007). Preparation of a copper-based fluorescent probe for nitric oxide and its use in mammalian cultured cells. Nat. Protoc. 2, 408–415.

Lowes, M.A., Chamian, F., Abello, M.V., Fuentes-Duculan, J., Lin, S.-L., Nussbaum, R., Novitskaya, I., Carbonaro, H., Cardinale, I., Kikuchi, T., et al. (2005). Increase in TNF-alpha and inducible nitric oxide synthase-expressing dendritic cells in psoriasis and reduction with efalizumab (anti-CD11a). Proc. Natl. Acad. Sci. U. S. A. 102, 19057–19062.

Ma, D.Y., and Clark, E.A. (2009). The role of CD40 and CD40L in Dendritic Cells. Semin. Immunol. 21, 265–272.

Mackey, M.F., Barth, R.J., and Noelle, R.J. (1998). The role of CD40/CD154 interactions in the priming, differentiation, and effector function of helper and cytotoxic T cells. J. Leukoc. Biol. 63, 418–428.

MacMicking, J., Xie, Q.W., and Nathan, C. (1997). Nitric oxide and macrophage function. Annu. Rev. Immunol. 15, 323–350.

Mantovani, A., Sozzani, S., Locati, M., Allavena, P., and Sica, A. (2002). Macrophage polarization: tumor-associated macrophages as a paradigm for polarized M2 mononuclear phagocytes. Trends Immunol. 23, 549–555.

Marigo, I., Bosio, E., Solito, S., Mesa, C., Fernandez, A., Dolcetti, L., Ugel, S., Sonda, N., Bicciato, S., Falisi, E., et al. (2010). Tumor-induced tolerance and immune suppression depend on the C/EBPbeta transcription factor. Immunity 32, 790–802.

Matsuda, H., and Iyanagi, T. (1999). Calmodulin activates intramolecular electron transfer between the two flavins of neuronal nitric oxide synthase flavin domain. Biochim. Biophys. Acta 1473, 345–355.

Melero, I., Gaudernack, G., Gerritsen, W., Huber, C., Parmiani, G., Scholl, S., Thatcher, N., Wagstaff, J., Zielinski, C., Faulkner, I., et al. (2014a). Therapeutic vaccines for cancer: an overview of clinical trials. Nat. Rev. Clin. Oncol. 11, 509–524.

Melero, I., Rouzaut, A., Motz, G.T., and Coukos, G. (2014b). T-cell and NK-cell infiltration into solid tumors: a key limiting factor for efficacious cancer immunotherapy. Cancer Discov. 4, 522–526.

Mellman, I., Coukos, G., and Dranoff, G. (2011). Cancer immunotherapy comes of age. Nature 480, 480–489.

Miguel, R.D.V., Cherpes, T.L., Watson, L.J., and McKenna, K.C. (2010). CTL Induction of Tumoricidal Nitric Oxide Production by Intratumoral Macrophages Is Critical for Tumor Elimination. J. Immunol. 185, 6706–6718.

Mittendorf, E.A., Clifton, G.T., Holmes, J.P., Clive, K.S., Patil, R., Benavides, L.C., Gates, J.D., Sears, A.K., Stojadinovic, A., Ponniah, S., et al. (2012). Clinical

trial results of the HER-2/neu (E75) vaccine to prevent breast cancer recurrence in high-risk patients: from US Military Cancer Institute Clinical Trials Group Study I-01 and I-02. Cancer 118, 2594–2602.

Molon, B., Ugel, S., Del Pozzo, F., Soldani, C., Zilio, S., Avella, D., De Palma, A., Mauri, P., Monegal, A., Rescigno, M., et al. (2011). Chemokine nitration prevents intratumoral infiltration of antigen-specific T cells. J. Exp. Med. 208, 1949–1962.

Moncada, S., Palmer, R.M., and Higgs, E.A. (1991). Nitric oxide: physiology, pathophysiology, and pharmacology. Pharmacol. Rev. 43, 109–142.

Murray, P.J., Allen, J.E., Biswas, S.K., Fisher, E.A., Gilroy, D.W., Goerdt, S., Gordon, S., Hamilton, J.A., Ivashkiv, L.B., Lawrence, T., et al. (2014). Macrophage activation and polarization: nomenclature and experimental guidelines. Immunity 41, 14–20.

Nagano, T., and Yoshimura, T. (2002). Bioimaging of nitric oxide. Chem. Rev. 102, 1235–1270.

Nagaraj, S., Gupta, K., Pisarev, V., Kinarsky, L., Sherman, S., Kang, L., Herber, D., Schneck, J., and Gabrilovich, D.I. (2007). Altered recognition of antigen is a novel mechanism of CD8+ T cell tolerance in cancer. Nat. Med. 13, 828–835.

Nosho, K., Baba, Y., Tanaka, N., Shima, K., Hayashi, M., Meyerhardt, J.A., Giovannucci, E., Dranoff, G., Fuchs, C.S., and Ogino, S. (2010). Tumour-infiltrating T-cell subsets, molecular changes in colorectal cancer and prognosis: cohort study and literature review. J. Pathol. 222, 350–366.

Ogino, S., Nosho, K., Kirkner, G.J., Kawasaki, T., Meyerhardt, J.A., Loda, M., Giovannucci, E.L., and Fuchs, C.S. (2009). CpG island methylator phenotype, microsatellite instability, BRAF mutation and clinical outcome in colon cancer. Gut 58, 90–96.

Pacher, P., Beckman, J.S., and Liaudet, L. (2007). Nitric Oxide and Peroxynitrite in Health and Disease. Physiol. Rev. 87, 315–424.

Pinchuk, L.M., Polacino, P.S., Agy, M.B., Klaus, S.J., and Clark, E.A. (1994). The role of CD40 and CD80 accessory cell molecules in dendritic cell-dependent HIV-1 infection. Immunity 1, 317–325.

Polanska, U.M., and Orimo, A. (2013). Carcinoma-associated fibroblasts: non-neoplastic tumour-promoting mesenchymal cells. J. Cell. Physiol. 228, 1651–1657.

Predonzani, A., Calì, B., Agnellini, A.H., and Molon, B. (2015). Spotlights on immunological effects of reactive nitrogen species: When inflammation says nitric oxide. World J. Exp. Med. 5, 64–76.

Restifo, N.P., Esquivel, F., Kawakami, Y., Yewdell, J.W., Mulé, J.J., Rosenberg, S.A., and Bennink, J.R. (1993). Identification of human cancers deficient in antigen processing. J. Exp. Med. 177, 265–272.

Restifo, N.P., Dudley, M.E., and Rosenberg, S.A. (2012). Adoptive immunotherapy for cancer: harnessing the T cell response. Nat. Rev. Immunol. 12, 269–281.

Robbins, P.F., Morgan, R.A., Feldman, S.A., Yang, J.C., Sherry, R.M., Dudley, M.E., Wunderlich, J.R., Nahvi, A.V., Helman, L.J., Mackall, C.L., et al. (2011). Tumor Regression in Patients With Metastatic Synovial Cell Sarcoma and Melanoma Using Genetically Engineered Lymphocytes Reactive With NY-ESO-1. J. Clin. Oncol. 29, 917–924.

Rosenberg, S.A., and Restifo, N.P. (2015). Adoptive cell transfer as personalized immunotherapy for human cancer. Science 348, 62–68.

Rosenberg, S.A., Spiess, P., and Lafreniere, R. (1986). A new approach to the adoptive immunotherapy of cancer with tumor-infiltrating lymphocytes. Science 233, 1318–1321.

Rosenberg, S.A., Yang, J.C., Sherry, R.M., Kammula, U.S., Hughes, M.S., Phan, G.Q., Citrin, D.E., Restifo, N.P., Robbins, P.F., Wunderlich, J.R., et al. (2011). Durable complete responses in heavily pretreated patients with metastatic melanoma using T-cell transfer immunotherapy. Clin. Cancer Res. Off. J. Am. Assoc. Cancer Res. 17, 4550–4557.

Sallusto, F., and Lanzavecchia, A. (1994). Efficient presentation of soluble antigen by cultured human dendritic cells is maintained by granulocyte/macrophage colony-stimulating factor plus interleukin 4 and downregulated by tumor necrosis factor alpha. J. Exp. Med. 179, 1109–1118.

Schmid, M., Wege, A.K., and Ritter, U. (2012). Characteristics of "Tip-DCs and MDSCs" and their potential role in leishmaniasis. Microb. Immunol. 3, 74.

Schreiber, R.D., Old, L.J., and Smyth, M.J. (2011). Cancer immunoediting: integrating immunity's roles in cancer suppression and promotion. Science 331, 1565–1570.

Scott, A.M., Wolchok, J.D., and Old, L.J. (2012). Antibody therapy of cancer. Nat. Rev. Cancer 12, 278–287.

Segal, N.H., Parsons, D.W., Peggs, K.S., Velculescu, V., Kinzler, K.W., Vogelstein, B., and Allison, J.P. (2008). Epitope landscape in breast and colorectal cancer. Cancer Res. 68, 889–892.

Serbina, N.V., Salazar-Mather, T.P., Biron, C.A., Kuziel, W.A., and Pamer, E.G. (2003). TNF/iNOS-producing dendritic cells mediate innate immune defense against bacterial infection. Immunity 19, 59–70.

Sherman, M.H., Downes, M., and Evans, R.M. (2012). Nuclear receptors as modulators of the tumor microenvironment. Cancer Prev. Res. Phila. Pa 5, 3–10.

Shiao, S.L., Ganesan, A.P., Rugo, H.S., and Coussens, L.M. (2011). Immune microenvironments in solid tumors: new targets for therapy. Genes Dev. 25, 2559–2572.

Sica, A., and Mantovani, A. (2012). Macrophage plasticity and polarization: in vivo veritas. J. Clin. Invest. 122, 787–795.

Smith-Garvin, J.E., Koretzky, G.A., and Jordan, M.S. (2009). T cell activation. Annu. Rev. Immunol. 27, 591–619.

Steinert, J.R., Robinson, S.W., Tong, H., Haustein, M.D., Kopp-Scheinpflug, C., and Forsythe, I.D. (2011). Nitric oxide is an activity-dependent regulator of target neuron intrinsic excitability. Neuron 71, 291–305.

Summers deLuca, L., Ng, D., Gao, Y., Wortzman, M.E., Watts, T.H., and Gommerman, J.L. (2011). LTβR signaling in dendritic cells induces a type I IFN response that is required for optimal clonal expansion of CD8+ T cells. Proc. Natl. Acad. Sci. U. S. A. 108, 2046–2051.

Tengan, C.H., Rodrigues, G.S., and Godinho, R.O. (2012). Nitric Oxide in Skeletal Muscle: Role on Mitochondrial Biogenesis and Function. Int. J. Mol. Sci. 13, 17160–17184.

Topalian, S.L., Weiner, G.J., and Pardoll, D.M. (2011). Cancer Immunotherapy Comes of Age. J. Clin. Oncol. 29, 4828–4836.

Ugel, S., De Sanctis, F., Mandruzzato, S., and Bronte, V. (2015). Tumor-induced myeloid deviation: when myeloid-derived suppressor cells meet tumor-associated macrophages. J. Clin. Invest. 125, 3365–3376.

Van Cutsem, E., Köhne, C.-H., Hitre, E., Zaluski, J., Chang Chien, C.-R., Makhson, A., D'Haens, G., Pintér, T., Lim, R., Bodoky, G., et al. (2009). Cetuximab and Chemotherapy as Initial Treatment for Metastatic Colorectal Cancer. N. Engl. J. Med. 360, 1408–1417.

Weigert, A., and Brüne, B. (2008). Nitric oxide, apoptosis and macrophage polarization during tumor progression. Nitric Oxide Biol. Chem. Off. J. Nitric Oxide Soc. 19, 95–102.

Weng, W.-K., and Levy, R. (2003). Two immunoglobulin G fragment C receptor polymorphisms independently predict response to rituximab in patients with follicular lymphoma. J. Clin. Oncol. Off. J. Am. Soc. Clin. Oncol. 21, 3940–3947.

Wolin, M.S. (2009). Reactive oxygen species and the control of vascular function. Am. J. Physiol. - Heart Circ. Physiol. 296, H539–H549.

Abbreviations

ACT: adoptive cell therapy
ADAM17: disintegrin and metalloproteinase domain-containing protein 17
ADCC: antibody-dependent cellular cytotoxicity
APCs: antigen-presenting cells
ARG1: arginase 1
CAFs: cancer associated fibroblasts
CAR: chimaeric antigen receptor therapy
CDC: complement-dependent cytotoxicity
cDCs: conventional DCs
CDP: common DC progenitors
cNOS: constitutive nitric oxide sintase
DCs: dendritic cells
eNOS or NOS3: endothelial nitric oxide synthase
FGFs: fibroblasts growth factors
GAL-9: galectin-9
GM-CSF: granulocyte macrophage colony stimulating factor
HGF: hepatocyte growth factor
HPLC: High Performance Liquid Chromatography
IL-1: interleukin-1
IL-2: interleukin 2
INF-γ: interferon gamma
iNOS or NOS2: inducible nitric oxide synthase
LPS: lipopolysaccharide
mAbs: monoclonal antibodies
MDP: macrophage/DC progenitor
MDSCs: myeloid derived suppressor cells
MHC: major histocompatibility complex proteins
mtNOS: mithocondrial NO synthase
NK: natural killer
NKT: natural killer T cells
nNOS or NOS1: neural nitri oxide synthase
NO: nitric oxide
NOS: nitric oxide synthases
PAP: prostatic acid phosphatase
PARP: Poly (ADP-ribose) polymerase
pDCs: plasmacytoid DCs
PDGFs: platelet-derived growth factors
RECIST: response evaluation criteria in solid tumors
ROI: region of interest
RNOS: reactive nitrogen oxide species
RNS: reactive nitrogen species
ROS: reactive oxygen species
sCD40L: recombinant soluble CD40L
SDF1: stromal cell-derived factor 1

SOD: superoxide dismutase
TAAs: tumor-associated antigens
TAMs: tumor-associated macrophages
TCR: T cell receptor
TIL: tumor infiltrating lymphocyte
Tip-DCs: TNF/iNOS producing dendritic cells
TLS: tertiary lymphoid structures
TNFRSF Tumor Necrosis Factor Receptor superfamily
T_{reg}: regulatory T cells
VEGF: vascular endothelial growth factors

Pubblications

Calì, B., Ceolin, S., Ceriani, F., Bortolozzi, M., Agnellini, A.H.R., Zorzi, V., Predonzani, A., Bronte, V., Molon, B., and Mammano, F. (2015). Critical role of gap junction communication, calcium and nitric oxide signaling in bystander responses to focal photodynamic injury. Oncotarget 6, 10161–10174.

Predonzani, A., Calì, B., Agnellini, A.H., and Molon, B. (2015). Spotlights on immunological effects of reactive nitrogen species: When inflammation says nitric oxide. World J. Exp. Med. 5, 64–76.